Revisiting the Lyth bound constraints on inflation from ACT DR6 results*

Rui Yang (杨睿)† Jun Tao (陶军)‡ Peng Wang (王鹏)§ Mian Zhu (朱勉)¶

College of Physics, Sichuan University, Chengdu 610065, China

Abstract: The Lyth bound states that the field excursion of the inflaton must be sub-Planckian, thereby imposing an upper bound on the amplitude of the tensor power spectrum in inflationary scenarios. This bound is conventionally derived under the assumption of a scale-invariant curvature power spectrum, *i.e.*, $n_s = 1$. However, astrophysical observations confirm a red-tilted spectrum with $n_s < 1$. In light of recent results from the Atacama Cosmology Telescope (ACT) DR6, we revisit these constraints using the newly inferred scalar spectral index, $n_s \simeq 0.9743$. Incorporating the ACT data yields a different upper bound on the tensor-to-scalar ratio r and clarifies whether non-canonical inflationary scenarios can remain compatible with both CMB observations and a sub-Planckian field excursion. Our result highlights the importance of combining theoretical considerations of the Lyth bound with up-to-date astrophysical data.

Keywords: Inflation, Lyth bound, ACT DR6

DOI: 10.1088/1674-1137/ae9b9c **CSTR:** 32044.14.ChinesePhysicsC.51015102

I. INTRODUCTION

Inflation is the leading paradigm for the primordial universe [1−7]. Nevertheless, inflation faces conceptual challenges. A central challenge is the so-called Lyth bound [8], which calls into question the consistency of an effective field theory description of inflation. The Lyth bound states that the field excursion $\Delta\phi$ is related to the tensor-to-scalar ratio r and the e-folding number N_* via

$$\Delta\phi/M_p \simeq \left(\frac{r}{0.002}\right)^{\frac{1}{2}} \left(\frac{N_*}{60}\right) , \tag{1}$$

in canonical inflation. As a result, the field excursion over the entire inflationary period can exceed the Planck mass when $r \geq 0.002$. This implies that the effective description is sensitive to higher-dimensional operators unless the large field range is protected by a symmetry or by a suitable ultraviolet completion. Extensive literature has investigated the implications of the Lyth bound and possible ways to circumvent it [9−31]. See, e.g., [32] for a review.

Conventionally, the Lyth bound is evaluated by assuming a scale-invariant curvature power spectrum P_ζ, *i.e.*, a scalar spectral index $n_s = 1$. However, observations suggest a slight red tilt in P_ζ. For example, the Planck 2018 results suggest [33]

$$n_s = 0.9649 \pm 0.0042 . \tag{2}$$

When the red tilt is taken into consideration, the constraints imposed by the Lyth bound are modified [9, 34]. Notably, Refs. [35, 36] proposed that this red tilt strengthens the Lyth bound constraint. Therefore, it is essential to revisit the Lyth bound constraint by accounting for the red tilt. This task is especially timely given the recent Atacama Cosmology Telescope (ACT) result, as the ACT DR6 data imply a scalar spectral index slightly different from that reported by the Planck Collaboration [37]

$$n_s = 0.9743 \pm 0.0034 , \tag{3}$$

and has generated immediate interest in the cosmology community [38−71]. Hence, we are motivated to investigate the updated Lyth bound constraints using the new ACT DR6 data.

Because canonical single-field slow-roll inflation is severely constrained by the Lyth bound, we consider inflationary scenarios with non-canonical scalar-field kinet-

Received 18 June 2026; Accepted 17 August 2026; Accepted manuscript online 18 August 2026

* Supported by the National Natural Science Foundation of China (12175212, 12275183, 12503005), the Sichuan Science and Technology Program (2026NSFSC0804), and the Fundamental Research Funds for the Central Universities (YJ202551)

† E-mail: yangrui7@stu.scu.edu.cn

‡ E-mail: taojun@scu.edu.cn

§ E-mail: pengw@scu.edu.cn

¶ E-mail: zhumian@scu.edu.cn (corresponding author)

©2027 Chinese Physical Society and the Institute of High Energy Physics of the Chinese Academy of Sciences and the Institute of Modern Physics of the Chinese Academy of Sciences and IOP Publishing Ltd. All rights, including for text and data mining, AI training, and similar technologies, are reserved.

ic terms, which are constructed to evade the Lyth bound challenge [72−79]. Notably, the Lyth bound constraints on these non-canonical scenarios have been investigated almost exclusively under the assumption $n_s = 1$, and can therefore be improved by incorporating the ACT results, which is the focus of this manuscript. Specifically, we investigate two possible non-canonical couplings: one with a kinetic-inflaton coupling [80−84], and another with a modified kinetic term $K(X)$ [85−92]. We find that the combination of the sub-Planckian field excursion required by the Lyth bound and the red-tilted curvature spectrum suggested by ACT results can impose strengthened constraints on inflationary scenarios.

The manuscript is organized as follows. We introduce the concept of the Lyth bound pedagogically in Sec. II, and illustrate how a red-tilted curvature spectrum can strengthen this bound, using a kinetic-inflaton coupling model as an example. We then investigate inflationary scenarios with modified kinetic terms in Sec. III, and show that a certain class of models consistent with the PLANCK 2018 + Lyth bound joint constraints is excluded by the ACT + Lyth bound joint analysis. We finally conclude in Sec. IV.

II. A PEDAGOGICAL INTRODUCTION TO LYTH BOUND

A. The original Lyth bound

In a spatially flat Friedmann–Lemaître–Robertson–Walker (FLRW) universe

$$\mathrm{d}s^2 = a^2(\tau)\left[-\mathrm{d}\tau^2 + \delta_{ij}\mathrm{d}x^i\mathrm{d}x^j\right], \tag{4}$$

$$\frac{1}{M_p}\left|\frac{\mathrm{d}\phi}{\mathrm{d}N}\right| = \sqrt{2\epsilon}\,. \tag{5}$$

Moreover, the consistency relation implies $r = 16\epsilon$, so that

$$\frac{1}{M_p}\left|\frac{\mathrm{d}\phi}{\mathrm{d}N}\right| \simeq \sqrt{\frac{r}{8}}. \tag{6}$$

Thus, the canonical field excursion during inflation is

$$\frac{\Delta\phi}{M_p} \simeq \int_{N_{\rm bg}}^{N_{\rm end}} \mathrm{d}N \sqrt{\frac{r(N)}{8}}\,, \tag{7}$$

where $N_{\rm bg}$ and $N_{\rm end}$ denote the number of e-folds at the beginning and end of the time interval under consideration, respectively. For later convenience, let us introduce $N_\star \equiv N_{\rm end} - N_{\rm bg}$. We require the single-field description to remain valid at least from the CMB scale to the end of inflation. To solve the flatness and horizon problems, this interval is conventionally estimated to be $N_* \simeq 60$. Assuming a constant r over different values of N, the integral immediately yields the Lyth bound constraint in Eq. (1).

B. An example: Lyth bound with non-canonical kinetic terms

To demonstrate how the inclusion of non-canonical kinetic terms may modify the Lyth bound constraint, we begin with the following non-canonical action.

$$\mathcal{S} = \int \mathrm{d}^4x\sqrt{-g}\left[\frac{M_p^2}{2}R - \frac{1}{2}m^2(\phi)\partial^\mu\phi\partial_\mu\phi - V(\phi)\right], \tag{8}$$

and use the following choices [82]

$$m^2(\phi) = \left(\frac{\alpha^2-\tilde{\alpha}^2}{\tilde{\alpha}^2}\right)\frac{1}{1+\beta^2\mathrm{e}^{\alpha\phi/M_p}} + 1\,,\ V(\phi) = M_p^4\mathrm{e}^{-\alpha\phi/M_p}\,. \tag{9}$$

Here, the coupling $m^2(\phi)$ can reduce the field excursion relative to the canonical case for a given geometric evolution. Although we adopt the form of $m^2(\phi)$ following [82], any choice satisfying $m(\phi) \gg 1$ can, in principle, produce the same effect. In addition, the steep exponential potential [93] can render the field coordinate effectively invariant after canonical normalization and is therefore widely adopted in quintessential inflation. The associated Friedmann equations are

$$3M_p^2H^2 = \frac{1}{2}m^2(\phi)\dot{\phi}^2 + V(\phi)\,, \tag{10}$$

$$2M_p^2\dot{H} = -m^2(\phi)\dot{\phi}^2\,. \tag{11}$$

The field velocity in this case is

$$\frac{1}{M_p}\left|\frac{\mathrm{d}\phi}{\mathrm{d}N}\right| = \frac{\sqrt{2\epsilon}}{m(\phi)}\,. \tag{12}$$

Compared with Eq. (7), we find that $\Delta\phi$ can be modified by the function $m(\phi)$. Thus, an appropriately chosen $m(\phi)$ can reduce the value of $\Delta\phi$, thereby allowing a smaller field excursion for a fixed r [82]. Although this appears to circumvent the Lyth bound for the original field ϕ, such a conclusion is premature, as demonstrated in the following section.

C. Coordinate excursion versus canonical excursion

This apparent evasion, however, can be an artifact of field parametrization. Under a field redefinition $\phi \to f(\phi)$, the excursion changes, whereas the physics remains invariant. A commonly adopted approach in discussions of the Lyth bound is to measure the distance using the canonically normalized field [94]. In the model in Eq. (8),

this can be done naturally by introducing the canonically normalized field

$$\mathrm{d}\chi \equiv m(\phi)\mathrm{d}\phi\,. \tag{13}$$

However, after transforming to the canonical scalar field, the field range is simply

$$\frac{\Delta\chi}{M_p} = \int^{N_*} \mathrm{d}N\,\sqrt{r(N)/8}\,. \tag{14}$$

Thus, if the field excursion is interpreted as the canonical field excursion, the kinetic coupling to the inflaton does not enable the model to evade the constraints imposed by the Lyth bound.

Specifically, the excursion of ϕ in the model of Eq. (8) is

$$\frac{1}{M_p}\left|\frac{\mathrm{d}\phi}{\mathrm{d}N}\right| = \frac{\sqrt{2\epsilon}}{m(\phi)} = \frac{\alpha}{m^2(\phi)} = \frac{2\epsilon}{\alpha} = \frac{r}{8\alpha}\,. \tag{15}$$

where we used the expression for the slow-roll parameter $\epsilon \equiv -\dot{H}/H^2$

$$m(\phi(N_p))^2 \simeq \frac{8\alpha^2}{r}\,,\ \epsilon \simeq \frac{M_p^2}{2m^2(\phi)}\left(\frac{V'(\phi)}{V(\phi)}\right)^2 = \frac{\alpha^2}{2m^2(\phi)}\,, \tag{16}$$

and it is immediately apparent that a large α can significantly suppress $\Delta\phi$.

Moreover, we need to account for the effect of $n_s \neq 1$ on $\Delta\chi$. Again, the consistency relation gives

$$n_t \simeq -\frac{r}{8}\,,\ \delta \equiv 1 - n_s\,, \tag{17}$$

thus

$$\frac{\mathrm{d}\ln r}{\mathrm{d}N} \simeq n_t - (n_s - 1) = \delta - \frac{r}{8}\,. \tag{18}$$

Given the observed small red tilt, we adopt the approximation $r(N) \simeq r_* \mathrm{e}^{\delta N}$, where r_* is the tensor-to-scalar ratio at the ACT pivot scale, $k_* = 0.05\ \mathrm{Mpc}^{-1}$. This leads to

$$\Delta\chi/M_p \simeq \left(\frac{r_*}{8}\right)^{\frac{1}{2}}\frac{2}{\delta}\left(\mathrm{e}^{\delta N_*/2} - 1\right)\,, \tag{19}$$

which reduces to $\Delta\chi/M_p = N_*(r_*/8)^{1/2}$ in the limit $\delta \to 0$. Notably, the dependence of χ on α is now implicit. In addition, the inequality $\Delta\chi/M_p \ll 1$ implies

$$r_* \ll \frac{2\delta^2}{\left(\mathrm{e}^{\delta N_*/2} - 1\right)^2}\,. \tag{20}$$

Therefore, the upper bound on r_* cannot be adjusted by varying α once δ and N_* are fixed.

D. Improved Lyth bound constraints with ACT

Here, we do not intend to assess whether $\Delta\phi$ and $\Delta\chi$ are more appropriate for considerations of the Lyth bound. Instead, we show in this section that precise measurements of n_s and r are essential for constraining the Lyth bound and that the model can be constrained through a joint analysis of the Lyth bound and ACT observations. The model in Eq. (8) is designed to suppress the coordinate excursion and thereby evade the usual Lyth bound constraint. Thus, the Lyth bound enters the scenario at the level of model construction. Nevertheless, once the action is specified based on the Lyth bound consideration, its predictions for (n_s, r) cannot be consistent with ACT observations, as shown below. For the canonical field excursion case, we derive the upper bound on r from Eq. (20) for three cases: $n_s = 1$, $n_s = 0.9649$ (Planck 2018), and $n_s = 0.9743$ (ACT DR6). The results are summarized in Table 1. We find that the Lyth bound becomes more stringent as the deviation of n_s from unity increases. The Planck 2018 results impose the strictest upper bound, $r < 7.1\times10^{-4}$ for $N_* = 60$, whereas the ACT results slightly alleviate this constraint, allowing $r \lesssim 9.7\times10^{-4}$, because the suggested value of n_s is slightly larger than that from the Planck result.

Table 1. Upper limit on r from the Lyth bound for different assumed values of n_s.

N_*	$\delta \to 0\, n_s = 1$	Planck 2018 $n_s = 0.9649$	ACT DR6 $n_s = 0.9743$
50	3.20×10^{-3}	1.25×10^{-3}	1.63×10^{-3}
60	2.22×10^{-3}	7.07×10^{-4}	9.78×10^{-4}
70	1.63×10^{-3}	4.22×10^{-4}	6.21×10^{-4}
80	1.25×10^{-3}	2.61×10^{-4}	4.10×10^{-4}

We now consider the original field excursion $\Delta\phi$. Although the model permits a small $\Delta\phi$ for $\alpha \gg 1$, an internal consistency relation between n_s and r could render the model problematic. In the slow-roll approximation,

$$A_s = \frac{H^2}{8\pi^2 M_p^2 \epsilon},\ n_s - 1 = -2\epsilon - \eta,\ r = 16\epsilon, \tag{21}$$

where $\eta \equiv \dot{\epsilon}/H\epsilon$ is the second slow-roll parameter. Using the Friedmann equations and the slow-roll condition, we obtain

$$\eta(r) \simeq \frac{(8\alpha^2 - r)(r - 8\tilde{\alpha}^2)}{64(\alpha^2 - \tilde{\alpha}^2)}\,. \tag{22}$$

Expressing n_s in terms of η yields the following consistency relation

$$r(n_s) = 8\left[\alpha^2 - \sqrt{(\alpha^2-\tilde{\alpha}^2)\left(\alpha^2-(1-n_s)\right)}\right] , \quad (23)$$

In the large-α limit, which is required for a small $\Delta\phi$, Eq. (23) reduces to

$$r \simeq 4(\tilde{\alpha}^2+\delta) \geq 4\delta . \quad (24)$$

The ACT results imply $\delta = 0.0257$ and therefore $r \geq 0.103$, which far exceeds the upper limit set by the ACT observations. We perform both a semi-analytic investigation using the slow-roll approximation and a full numerical evaluation, as summarized in Fig. 1. The small differences between the semi-analytic and numerical results mainly arise from the slow-roll approximation used in the semi-analytic calculation, whereas the numerical calculation retains the full time evolution of the background and perturbations. The lower bound on r from Eq. (23) indeed prevents the model from being consistent with the ACT observations. The numerical and semi-analytic (n_s, r) values plotted in both panels of Fig. 1 are listed in Tables A1−A4 and A5−A8 of Appendix A.

The preceding discussion shows that the deviation of n_s from unity can significantly affect the constraints imposed by the Lyth bound. In particular, a joint analysis of the Lyth bound and the observed (n_s, r) values from CMB data can substantially strengthen constraints on inflationary models. Specifically, we show that the model (8), which was designed to evade the theoretical constraint from the Lyth bound, fails to pass the ACT test.

III. INFLATION WITH MODIFIED KINETIC TERMS

We now consider the inflationary scenario with modified kinetic terms. We adopt the following Lagrangian

$$P(X,\phi) = \mathcal{K}(X) - V(\phi) , \; X \equiv -\frac{1}{2} g^{\mu\nu}\partial_\mu\phi\,\partial_\nu\phi . \quad (25)$$

In a homogeneous background, $X = \dot{\phi}^2/2$. The tensor-to-scalar ratio r can be suppressed by using a power-law parametrization of $K(X)$

$$\mathcal{K}(X) = M^4\left(\frac{X}{M^4}\right)^\gamma , \; \gamma \geq 1 , \quad (26)$$

because the sound speed of curvature fluctuations is modified to

$$c_s^2 \equiv \frac{P_{,X}}{P_{,X}+2XP_{,XX}} = \frac{1}{2\gamma-1} < 1 , \quad (27)$$

and, as a result, the consistency relation $r \simeq 16 c_s \epsilon$ implies a smaller r for the same slow-roll parameter. The power-law parametrization in Eq. (26) is a representative model for the k-inflation scenario, as it keeps the sound speed constant. In particular, since $r \propto c_s$, reducing c_s can help suppress r, motivating phenomenological interest in investigating such models.

Let us explain why the model in Eq. (26) is expected to significantly modify the field excursion. For illustrative purposes, we use an exponential potential [93]

$$V(\phi) = V_0 \exp\left[-\lambda\left(\frac{\phi}{M_p}\right)^n\right] , \quad (28)$$

where M is a parameter with dimensions of mass. The slow-roll condition can be satisfied for $\lambda > 0$ and $n > 0$, with the slow-roll parameter given by

$$\epsilon \equiv -\frac{\dot{H}}{H^2} = \frac{XP_{,X}}{M_p^2H^2} = \frac{\gamma X^\gamma}{M_p^2H^2(M^4)^{\gamma-1}} . \quad (29)$$

Without loss of generality, we take $\phi > 0$; the field excursion is

$$\frac{1}{M_p}\frac{\mathrm{d}\phi}{\mathrm{d}N} = \sqrt{2}\left(\frac{\epsilon}{\gamma}\right)^{1/(2\gamma)}\left(\frac{M}{M_p}\right)^{1-1/\gamma}\left(\frac{H}{M}\right)^{1/\gamma-1} . \quad (30)$$

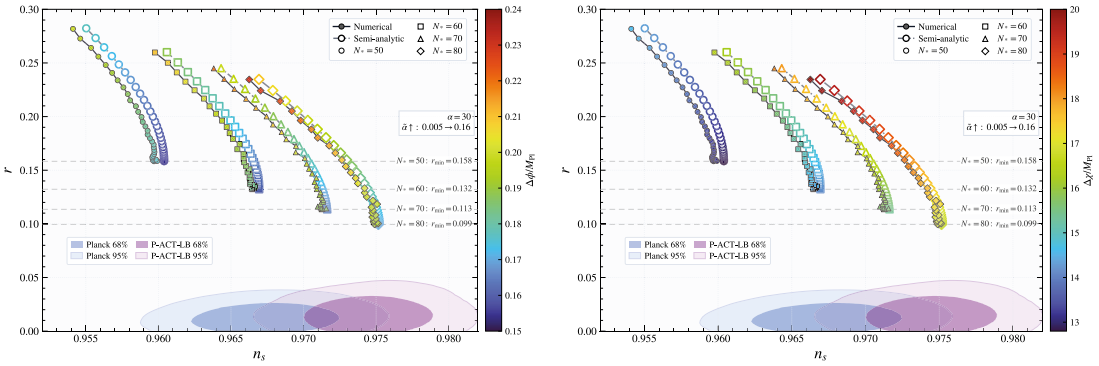


Fig. 1. (color online) The (n_s, r) plot is shown for model parameter $\alpha = 30$ and $N_* = 50, 60, 70, 80$. The model parameter is chosen such that $A_s = 2.1\times10^{-9}$ is fixed. The numerical and semi-analytic (n_s, r) values are listed in Tables A1−A4 and A5−A8 of Appendix A. The left and right panels show the coordinate and canonical field excursions, $\Delta\phi$ and $\Delta\chi$, respectively, indicating that the canonical field excursion is far beyond the Planck scale.

It is immediately apparent that the tensor-to-scalar ratio r cannot, by itself, determine the field excursion. In particular, in the limit $\gamma \gg 1$, the field excursion reduces to

$$\frac{1}{M_p}\frac{\mathrm{d}\phi}{\mathrm{d}N} \simeq \sqrt{2}\frac{M^2}{M_p H}\,, \tag{31}$$

which is completely decoupled from r. Thus, these models are expected to bypass the Lyth bound constraints through a substantial modification of the $\Delta\phi$-r relation [87, 88].

So far, the discussion has been based on the original field excursion, while a canonically normalized field cannot be introduced in the same way as in Sec. II.C. The model (26) is genuinely nonlinear in X, and there is, in general, no global field redefinition $\phi \to \chi(\phi)$ that transforms the full Lagrangian into a canonical form. Therefore, we use the original field excursion $\Delta\phi$ as a reference to analyze the Lyth bound constraint.

To examine whether the model in Eq. (25) can indeed bypass the Lyth bound constraint while remaining consistent with ACT observations, we evaluate (n_s, r) and $\Delta\phi$ for different model parameters, both semi-analytically under the slow-roll approximation and numerically, Tables B25−B48 of Appendix B list the semi-analytic results shown in the left panel of Fig. 2, while Tables B1−B24 list the numerical results shown in the right panel. The origin of the small difference between the semi-analytical and numerical results is the same as that discussed for Model I. The results show that ACT data, compared with Planck data, actually strengthen the Lyth bound constraint, in contrast to the case study in Sec. II.D. In particular, there exists a parameter space that fits the Planck data well while being marginally consistent with the Lyth bound, *i.e.*, $\Delta\phi/M_p \simeq 1$. However, the field excursion $\Delta\phi/M_p$ must exceed unity to be consistent with ACT observations in this model. Thus, the update from ACT measurements puts models that were originally consistent with Planck under tension.

One may wonder whether an extreme choice of parameters can restore the viability of the model. To discuss this possibility, we analyze the effects of the model parameters on n_s, r, and $\Delta\phi$. First, the e-folding number N has a critical impact on the values of n_s and r: increasing N enhances n_s while keeping r almost constant, at the cost of increasing $\Delta\phi$. When γ is of order 10, N must approach 80 to satisfy the ACT observations. However, in this case, $\Delta\phi/M_p$ already exceeds 1.5; thus, changing N does not help substantially.

We also find that varying n and V_0 has only a limited effect on the results. Increasing n leads to a slight change in n_s, whereas increasing V_0 primarily helps satisfy the Lyth-bound constraint, with only a limited effect on the ACT constraint. The value of M has a negligible impact on the results, as shown in the left panel of Fig. 3. The sensitivity to N_* is more significant: increasing N_* can move n_s toward the ACT-preferred value, but this shift is accompanied by a larger accumulated field excursion. Thus, the conclusion is not driven by a single fiducial choice of N_*.

Given this negative result, it is natural to ask whether γ, the most important parameter in these models, can improve the robustness of the model. As discussed above, increasing γ can both suppress r and substantially change $\Delta\phi$, so one may expect a larger γ to help evade the Lyth-bound and ACT constraints. Nonetheless, γ cannot be arbitrarily large. The effective field theory of inflation suggests $c_s \gg 0.003$ to avoid a strong-coupling problem [74], while observational constraints on primordial non-Gaussianities imply $c_s \geq 0.021$ (for the DBI inflation model, the constraint can be even more severe) [95]. In particular, the strong coupling scale of the Goldstone EFT behaves as

$$\Lambda_{\rm sc}^4 \simeq \frac{16\pi^2 M_p^2 |\dot{H}| c_s^5}{1-c_s^2}\,, \tag{32}$$

up to coefficients of order unity. Combining this estimate with $A_s = H^2/(8\pi^2 M_p^2 \epsilon c_s)$ yields

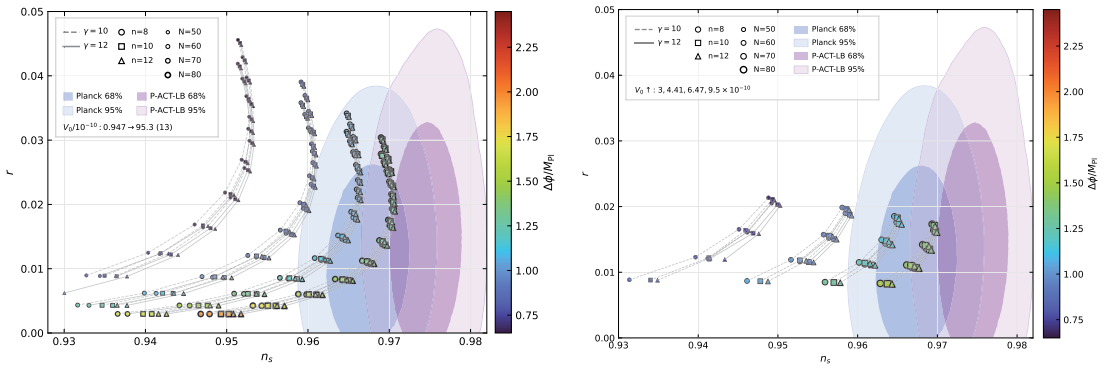


Fig. 2. (color online) Left panel: semi-analytic results for (n_s, r) and $\Delta\phi$ based on Eq. (30), whose validation assumes the slow-roll approximation. Right panel: numerical results obtained by directly evolving ζ for comparison. Again, the model parameter is chosen such that $A_s = 2.1\times10^{-9}$ is fixed. The semi-analytic results in the left panel are listed in Tables B25−B48 of Appendix B; the numerical results in the right panel are listed in Tables B1−B24. The color bar denotes the original field excursion $\Delta\phi/M_p$.

$$\left(\frac{H}{\Lambda_{\rm sc}}\right)^4 \simeq \frac{A_s}{2}\frac{1-c_s^2}{c_s^4}\,, \tag{33}$$

Thus, $c_s \gtrsim 0.1$ keeps $H/\Lambda_{\rm sc} \ll 1$, whereas reducing the sound speed substantially would make the EFT interpretation less robust and enhance equilateral non-Gaussianities. Therefore, we adopt $\gamma \lesssim 50$ to ensure $c_s \geq 0.1$.

In light of this discussion, we vary the parameter γ while keeping n, V_0, and N fixed, and present the corresponding values of n_s, r, and $\Delta\phi$ in the data for the $n = 10$ branch in the right panel of Fig. 3 are listed in Table B49 of Appendix B. Interestingly, a lower bound on $\Delta\phi$ that exceeds M_p emerges when γ is varied, suggesting that changing γ alone cannot circumvent the Lyth bound constraints.

The emergence of a lower bound can be explained as follows. To demonstrate this, we evaluate $\mathrm{d}\Delta\phi/\mathrm{d}\gamma$. The starting point is

$$\frac{\mathrm{d}\Delta\phi}{\mathrm{d}\gamma} = \frac{\mathrm{d}\phi_{\rm end}}{\mathrm{d}\gamma} - \frac{\mathrm{d}\phi_*}{\mathrm{d}\gamma}\,. \tag{34}$$

The right-hand side is determined by taking the total derivatives of the constraints.

$$P_\zeta(\phi_*,\gamma,\lambda) = A_s\,,\ \epsilon(\phi_{\rm end},\gamma,\lambda) = 1\,. \tag{35}$$

Because N_* is fixed, an additional constraint must be considered.

$$\int_{\phi_*}^{\phi_{\rm end}} \left[\frac{\mathrm{d}\phi}{\mathrm{d}N}(\gamma,\lambda)\right]^{-1} \mathrm{d}\phi = N_*\,. \tag{36}$$

Substituting these expressions into Eq. (34), we obtain

$$\begin{aligned}\frac{\mathrm{d}\Delta\phi}{\mathrm{d}\gamma} &= D_\gamma + C_\lambda\frac{\mathrm{d}\lambda}{\mathrm{d}\gamma}, \quad D_\gamma = -\frac{\partial_\gamma\epsilon}{\partial_{\phi_{\rm end}}\epsilon} + \frac{\partial_\gamma P_s}{\partial_{\phi_*}P_s}\,,\\ C_\lambda &= -\frac{\partial_\lambda\epsilon}{\partial_{\phi_{\rm end}}\epsilon} + \frac{\partial_\lambda P_s}{\partial_{\phi_*}P_s}\,.\end{aligned} \tag{37}$$

Note that P_s and ϵ are implicit functions defined by Eq. (35). Because a complete analytical treatment is intractable, we proceed with a numerical evaluation. We list the values of $\mathrm{d}\lambda/\mathrm{d}\gamma$, D_γ, and C_λ in Table 2. For this parameter choice, D_γ increases from negative values toward 0 as γ increases. In contrast, $C_\lambda\frac{\mathrm{d}\lambda}{\mathrm{d}\gamma}$ eventually becomes positive as γ increases. This behavior leads to a sign reversal in $\mathrm{d}\Delta\phi/\mathrm{d}\gamma$ and, consequently, to a local minimum in $\Delta\phi$ as γ is varied.

In this regard, the model may have difficulty simultaneously evading the Lyth-bound constraint and fitting the ACT observations by adjusting its parameters. We therefore reiterate that the joint consideration of the Lyth bound and ACT results can effectively constrain inflationary scenarios, placing models that are compatible with either constraint alone in tension.

IV. CONCLUSION

We have investigated how the most recent ACT observations shed new light on the physics of the Lyth bound. Although some inflationary models may remain viable under the original Lyth bound, the inclusion of a red tilt can strengthen the constraint and place such models in tension with observations. This is explicitly demonstrated by the kinetic-inflaton coupling model, which was designed to evade the Lyth-bound constraint: the Lyth bound motivates the construction of such a model, while the inclusion of the red tilt suggests that its predictions for (n_s, r) are incompatible with the ACT observations. We also investigated models with a modified kinetic term and found that they can satisfy the joint Planck 2018 and Lyth-bound constraints, but fail when the Planck 2018 data are replaced by the ACT data.

Given the abundance of inflationary models in the literature, an exhaustive investigation of all existing scenarios is not possible. The purpose of this manuscript is to highlight the power of jointly applying the theoretical Lyth-bound constraint and the most up-to-date CMB ob-

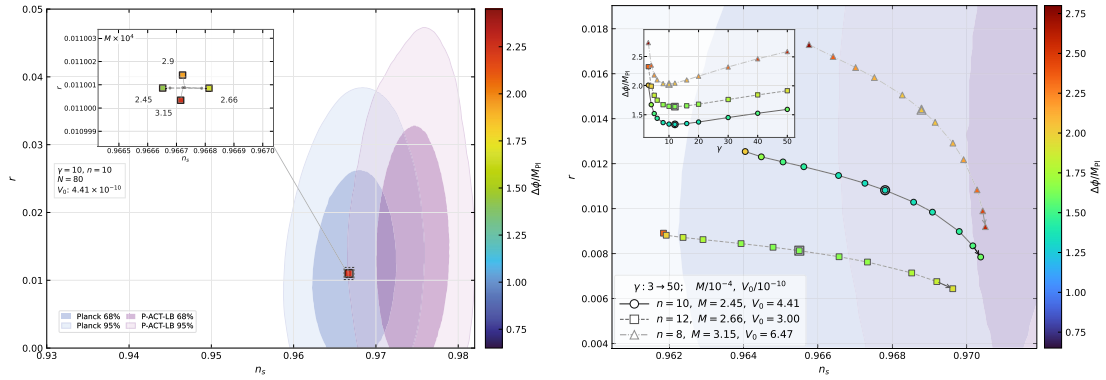


Fig. 3. (color online) Left panel: effects of M with the other parameters fixed. Right panel: effects of γ with the other parameters fixed. Again, λ is chosen so that $A_s = 2.1\times10^{-9}$ remains fixed. data for the $n = 10$ branch in the right panel are listed in Table B49 of Appendix B. $\Delta\phi/M_p$.

Table 2. Evolution of $\Delta\phi$ along the γ branch.

γ	$\mathrm{d}\lambda/\mathrm{d}\gamma$	D_γ	$C_\lambda \mathrm{d}\lambda/\mathrm{d}\gamma$	$\frac{\mathrm{d}\Delta\phi}{\mathrm{d}\gamma}$
1.5	$+1.5802\times10^{-10}$	−0.2733	−5.8120	−6.0853
6	$+1.6722\times10^{-7}$	−0.0324	−0.0280	−0.0605
8	-6.5174×10^{-9}	−0.0220	+0.00087	−0.0211
12	-7.7776×10^{-8}	−0.0135	+0.01393	+0.00042
50	-1.0290×10^{-9}	−0.00332	+0.00972	+0.00640

servations. We have already found this method to be powerful, and extending the formalism to other models in future work will be promising.

ACKNOWLEDGMENTS

We thank Yizhi Liang, Guohe Li and Jingming Pu for useful discussions and insightful suggestions.

APPENDIX A: DATA FOR FIGURE 1

This section summarizes the data underlying Fig. 1. We assume $\alpha = 30$ throughout. We present both the numerical results and the semi-analytical results obtained using the slow-roll approximation.

Table A1. Numerical, $N_* = 50$.

$\tilde{\alpha}$	β	n_s	r	$\Delta\phi/M_{\rm Pl}$
0.005	0.0019965	0.959698	0.158314	0.17575
0.010167	9.8189×10^{-4}	0.9599148	0.158631	0.175813
0.015333	6.5103×10^{-4}	0.9596259	0.159161	0.17592
0.0205	4.8700×10^{-4}	0.9598288	0.159903	0.176071
0.025667	3.8898×10^{-4}	0.9595938	0.160862	0.176265
0.030833	3.2379×10^{-4}	0.9595782	0.162039	0.176504
0.036	2.7730×10^{-4}	0.9596289	0.163435	0.176786
0.041167	2.4250×10^{-4}	0.9597029	0.165073	0.177114
0.046333	2.1544×10^{-4}	0.9597265	0.16693	0.177487
0.0515	1.9380×10^{-4}	0.9597131	0.169029	0.177905
0.056667	1.7608×10^{-4}	0.9596786	0.171356	0.17837
0.061833	1.6132×10^{-4}	0.9596713	0.173928	0.178881
0.067	1.4882×10^{-4}	0.9595635	0.176782	0.17944
0.072167	1.3809×10^{-4}	0.9594178	0.179896	0.180048
0.077333	1.2876×10^{-4}	0.959257	0.183246	0.180704
0.0825	1.2058×10^{-4}	0.9592558	0.186892	0.18141
0.087667	1.1335×10^{-4}	0.959105	0.190826	0.182167
0.092833	1.0689×10^{-4}	0.958918	0.195046	0.182976
0.098	1.0110×10^{-4}	0.9588355	0.199598	0.183838
0.10317	9.5838×10^{-5}	0.9586091	0.204426	0.184753
0.10833	9.1063×10^{-5}	0.9584491	0.209603	0.185724

Continued on next page

Table A1-continued from previous page

$\tilde{\alpha}$	β	n_s	r	$\Delta\phi/M_{\rm Pl}$
0.1135	8.6680×10^{-5}	0.9580546	0.215102	0.186751
0.11867	8.2650×10^{-5}	0.9578893	0.220986	0.187835
0.12383	7.8930×10^{-5}	0.9575895	0.227207	0.188977
0.129	7.5462×10^{-5}	0.9571911	0.233789	0.19018
0.13417	7.2232×10^{-5}	0.9568141	0.240767	0.191444
0.13933	6.9187×10^{-5}	0.9563682	0.24808	0.192771
0.1445	6.6338×10^{-5}	0.9558637	0.255919	0.194161
0.14967	6.3641×10^{-5}	0.9553566	0.264091	0.195618
0.15483	6.1077×10^{-5}	0.9546162	0.272711	0.197141
0.16	5.8644×10^{-5}	0.9541134	0.281792	0.198733

Table A2. Numerical, $N_* = 60$.

$\tilde{\alpha}$	β	n_s	r	$\Delta\phi/M_{\rm Pl}$
0.005	0.0016643	0.966458	0.132254	0.181873
0.010167	8.1847×10^{-4}	0.9664713	0.132573	0.18195
0.015333	5.4274×10^{-4}	0.9664267	0.133096	0.182079
0.0205	4.0596×10^{-4}	0.9666084	0.133848	0.18226
0.025667	3.2426×10^{-4}	0.9666834	0.134819	0.182494
0.030833	2.6991×10^{-4}	0.9665007	0.135997	0.182782
0.036	2.3116×10^{-4}	0.9662986	0.137408	0.183123
0.041167	2.0212×10^{-4}	0.9663092	0.139043	0.183519
0.046333	1.7957×10^{-4}	0.9663729	0.140906	0.183969
0.0515	1.6150×10^{-4}	0.9662816	0.143014	0.184476
0.056667	1.4672×10^{-4}	0.9662958	0.145379	0.185038
0.061833	1.3439×10^{-4}	0.9661421	0.148004	0.185658
0.067	1.2395×10^{-4}	0.9662681	0.150867	0.186336
0.072167	1.1498×10^{-4}	0.9660236	0.154034	0.187073
0.077333	1.0716×10^{-4}	0.9659099	0.157437	0.187871
0.0825	1.0032×10^{-4}	0.9658698	0.161158	0.18873
0.087667	9.4245×10^{-5}	0.9658656	0.165198	0.189653
0.092833	8.8815×10^{-5}	0.9654391	0.169543	0.19064
0.098	8.3916×10^{-5}	0.9655947	0.174162	0.191692
0.10317	7.9492×10^{-5}	0.9651278	0.17915	0.192812
0.10833	7.5437×10^{-5}	0.9649093	0.184487	0.194001
0.1135	7.1724×10^{-5}	0.9647045	0.190187	0.195261
0.11867	6.8296×10^{-5}	0.9643911	0.196231	0.196592
0.12383	6.5100×10^{-5}	0.9639767	0.20268	0.197998

Continued on next page

Table A2-continued from previous page

$\tilde{\alpha}$	β	n_s	r	$\Delta\phi/M_{\rm Pl}$
0.129	6.2126×10^{-5}	0.9635234	0.209528	0.19948
0.13417	5.9341×10^{-5}	0.9631319	0.216798	0.201039
0.13933	5.6712×10^{-5}	0.9624911	0.224482	0.202678
0.1445	5.4230×10^{-5}	0.9618636	0.232587	0.204399
0.14967	5.1878×10^{-5}	0.9612638	0.241177	0.206204
0.15483	4.9636×10^{-5}	0.9606458	0.250237	0.208094
0.16	4.7490×10^{-5}	0.9597546	0.259751	0.210072

Table A3. Numerical, $N_*=70$.

$\tilde{\alpha}$	β	n_s	r	$\Delta\phi/M_{\rm Pl}$
0.005	0.0014269	0.9712366	0.113558	0.187047
0.010167	7.0175×10^{-4}	0.97132	0.11387	0.187137
0.015333	4.6533×10^{-4}	0.971561	0.114407	0.187288
0.0205	3.4803×10^{-4}	0.9711759	0.115136	0.187501
0.025667	2.7798×10^{-4}	0.97098	0.116122	0.187775
0.030833	2.3139×10^{-4}	0.971168	0.117301	0.188112
0.036	1.9815×10^{-4}	0.9711718	0.118704	0.188512
0.041167	1.7325×10^{-4}	0.9713509	0.120346	0.188976
0.046333	1.5390×10^{-4}	0.971361	0.122229	0.189505
0.0515	1.3840×10^{-4}	0.9712575	0.124375	0.190099
0.056667	1.2571×10^{-4}	0.9710993	0.12674	0.190761
0.061833	1.1513×10^{-4}	0.9711663	0.129395	0.19149
0.067	1.0614×10^{-4}	0.9709109	0.132295	0.192289
0.072167	9.8424×10^{-5}	0.9708832	0.135527	0.193158
0.077333	9.1700×10^{-5}	0.9707583	0.139003	0.1941
0.0825	8.5788×10^{-5}	0.9708764	0.142781	0.195115
0.087667	8.0537×10^{-5}	0.9705913	0.146879	0.196207
0.092833	7.5844×10^{-5}	0.9703754	0.151318	0.197376
0.098	7.1585×10^{-5}	0.9702152	0.156076	0.198624
0.10317	6.7737×10^{-5}	0.9700848	0.16119	0.199954
0.10833	6.4201×10^{-5}	0.9694605	0.166674	0.201368
0.1135	6.0945×10^{-5}	0.9694781	0.172533	0.202868
0.11867	5.7933×10^{-5}	0.9688073	0.178806	0.204455
0.12383	5.5113×10^{-5}	0.9684896	0.185478	0.206134
0.129	5.2486×10^{-5}	0.9678934	0.192606	0.207905
0.13417	5.0008×10^{-5}	0.967451	0.200127	0.209772
0.13933	4.7665×10^{-5}	0.9667222	0.208133	0.211737
0.1445	4.5442×10^{-5}	0.9660383	0.216584	0.213802
0.14967	4.3328×10^{-5}	0.9652358	0.225555	0.215971
0.15483	4.1301×10^{-5}	0.9645316	0.234955	0.218245
0.16	3.9358×10^{-5}	0.9638125	0.244923	0.220627

Table A4. Numerical, $N_*=80$.

$\tilde{\alpha}$	β	n_s	r	$\Delta\phi/M_{\rm Pl}$
0.005	0.0012486	0.9749345	0.0994967	0.191528
0.010167	6.1406×10^{-4}	0.9748769	0.0997936	0.191631
0.015333	4.0720×10^{-4}	0.9751382	0.10032	0.191804
0.0205	3.0452×10^{-4}	0.9750585	0.101067	0.192047
0.025667	2.4324×10^{-4}	0.9748235	0.102031	0.192362
0.030833	2.0246×10^{-4}	0.9748628	0.10322	0.192749
0.036	1.7338×10^{-4}	0.9749764	0.104653	0.193208
0.041167	1.5157×10^{-4}	0.9747369	0.106292	0.193741
0.046333	1.3462×10^{-4}	0.9749534	0.108193	0.194348
0.0515	1.2107×10^{-4}	0.9747322	0.110342	0.195032
0.056667	1.0994×10^{-4}	0.9747838	0.112742	0.195793
0.061833	1.0065×10^{-4}	0.9746783	0.115428	0.196633
0.067	9.2773×10^{-5}	0.9750695	0.118377	0.197553
0.072167	8.5981×10^{-5}	0.9747734	0.121631	0.198557
0.077333	8.0068×10^{-5}	0.974352	0.125179	0.199645
0.0825	7.4854×10^{-5}	0.9742133	0.129012	0.200819
0.087667	7.0219×10^{-5}	0.9742017	0.133213	0.202083
0.092833	6.6064×10^{-5}	0.9737456	0.137734	0.203438
0.098	6.2290×10^{-5}	0.9735899	0.14261	0.204888
0.10317	5.8862×10^{-5}	0.9732477	0.147859	0.206433
0.10833	5.5711×10^{-5}	0.9729101	0.1535	0.208078
0.1135	5.2797×10^{-5}	0.9726439	0.159568	0.209826
0.11867	5.0083×10^{-5}	0.9721857	0.166022	0.211678
0.12383	4.7549×10^{-5}	0.9717663	0.172896	0.213638
0.129	4.5164×10^{-5}	0.9709781	0.18026	0.21571
0.13417	4.2913×10^{-5}	0.97054	0.188052	0.217895
0.13933	4.0774×10^{-5}	0.9697969	0.196347	0.220198
0.1445	3.8737×10^{-5}	0.9691955	0.205089	0.222622
0.14967	3.6791×10^{-5}	0.9683853	0.21437	0.225169
0.15483	3.4926×10^{-5}	0.9670413	0.224148	0.227842
0.16	3.3139×10^{-5}	0.9662573	0.234529	0.230645

Table A5. Semi-analytic, $N_*=50$.

$\tilde{\alpha}$	β	n_s	r	$\Delta\phi/M_{\rm Pl}$
0.005	0.0019753	0.9603924	0.158532	0.153928
0.010167	9.7147×10^{-4}	0.9603924	0.158846	0.153993
0.015333	6.4412×10^{-4}	0.960392	0.159374	0.154102
0.0205	4.8178×10^{-4}	0.960391	0.160119	0.154255
0.025667	3.8478×10^{-4}	0.9603889	0.161081	0.154452
0.030833	3.2029×10^{-4}	0.9603849	0.162265	0.154695
0.036	2.7430×10^{-4}	0.9603784	0.163672	0.154983

Continued on next page

Table A5-continued from previous page

$\tilde{\alpha}$	β	n_s	r	$\Delta\phi/M_{\rm Pl}$
0.041167	2.3984×10^{-4}	0.9603685	0.165307	0.155316
0.046333	2.1306×10^{-4}	0.9603539	0.167173	0.155695
0.0515	1.9163×10^{-4}	0.9603335	0.169276	0.15612
0.056667	1.7410×10^{-4}	0.960306	0.171622	0.156593
0.061833	1.5948×10^{-4}	0.9602699	0.174215	0.157113
0.067	1.4710×10^{-4}	0.9602235	0.177064	0.157682
0.072167	1.3646×10^{-4}	0.960165	0.180174	0.1583
0.077333	1.2723×10^{-4}	0.9600925	0.183553	0.158968
0.0825	1.1913×10^{-4}	0.960004	0.18721	0.159686
0.087667	1.1195×10^{-4}	0.9598974	0.191153	0.160457
0.092833	1.0555×10^{-4}	0.9597702	0.195392	0.16128
0.098	9.9798×10^{-5}	0.9596202	0.199936	0.162157
0.10317	9.4589×10^{-5}	0.9594447	0.204796	0.163088
0.10833	8.9845×10^{-5}	0.9592412	0.209981	0.164076
0.1135	8.5500×10^{-5}	0.9590068	0.215502	0.165121
0.11867	8.1499×10^{-5}	0.9587389	0.221372	0.166224
0.12383	7.7796×10^{-5}	0.9584344	0.227602	0.167387
0.129	7.4352×10^{-5}	0.9580905	0.234203	0.168611
0.13417	7.1136×10^{-5}	0.9577041	0.241187	0.169897
0.13933	6.8120×10^{-5}	0.9572721	0.248567	0.171247
0.1445	6.5280×10^{-5}	0.9567915	0.256356	0.172663
0.14967	6.2596×10^{-5}	0.9562592	0.264564	0.174145
0.15483	6.0050×10^{-5}	0.9556721	0.273206	0.175696
0.16	5.7627×10^{-5}	0.9550271	0.282292	0.177316

Table A6. Semi-analytic, $N_* = 60$.

$\tilde{\alpha}$	β	n_s	r	$\Delta\phi/M_{\rm Pl}$
0.005	0.0016488	0.9669395	0.132343	0.159955
0.010167	8.1088×10^{-4}	0.9669394	0.132657	0.160033
0.015333	5.3765×10^{-4}	0.966939	0.133186	0.160164
0.0205	4.0213×10^{-4}	0.9669378	0.133931	0.160348
0.025667	3.2117×10^{-4}	0.9669352	0.134895	0.160586
0.030833	2.6733×10^{-4}	0.9669305	0.136082	0.160878
0.036	2.2894×10^{-4}	0.9669227	0.137494	0.161224
0.041167	2.0017×10^{-4}	0.9669107	0.139137	0.161625
0.046333	1.7780×10^{-4}	0.9668932	0.141015	0.162083
0.0515	1.5990×10^{-4}	0.9668688	0.143135	0.162596
0.056667	1.4525×10^{-4}	0.9668359	0.145502	0.163167
0.061833	1.3303×10^{-4}	0.9667925	0.148124	0.163796
0.067	1.2267×10^{-4}	0.9667369	0.151009	0.164484
0.072167	1.1376×10^{-4}	0.9666669	0.154165	0.165233
0.077333	1.0602×10^{-4}	0.9665801	0.157602	0.166042

Continued on next page

Table A6-continued from previous page

$\tilde{\alpha}$	β	n_s	r	$\Delta\phi/M_{\rm Pl}$
0.0825	9.9223×10^{-5}	0.9664743	0.161329	0.166915
0.087667	9.3194×10^{-5}	0.9663467	0.165356	0.167851
0.092833	8.7805×10^{-5}	0.9661947	0.169694	0.168853
0.098	8.2949×10^{-5}	0.9660154	0.174355	0.169921
0.10317	7.8544×10^{-5}	0.9658059	0.17935	0.171058
0.10833	7.4521×10^{-5}	0.9655632	0.184692	0.172265
0.1135	7.0826×10^{-5}	0.9652839	0.190394	0.173544
0.11867	6.7412×10^{-5}	0.964965	0.196468	0.174896
0.12383	6.4242×10^{-5}	0.964603	0.202927	0.176323
0.129	6.1283×10^{-5}	0.9641946	0.209786	0.177828
0.13417	5.8509×10^{-5}	0.9637366	0.217057	0.179411
0.13933	5.5896×10^{-5}	0.9632254	0.224754	0.181076
0.1445	5.3425×10^{-5}	0.9626577	0.23289	0.182823
0.14967	5.1080×10^{-5}	0.9620303	0.24148	0.184655
0.15483	4.8846×10^{-5}	0.9613399	0.250534	0.186574
0.16	4.6711×10^{-5}	0.9605833	0.260067	0.188583

Table A7. Semi-analytic, $N_* = 70$.

$\tilde{\alpha}$	β	n_s	r	$\Delta\phi/M_{\rm Pl}$
0.005	0.0014149	0.9716292	0.113584	0.165059
0.010167	6.9585×10^{-4}	0.9716291	0.113898	0.165149
0.015333	4.6138×10^{-4}	0.9716286	0.114427	0.165302
0.0205	3.4509×10^{-4}	0.9716272	0.115173	0.165518
0.025667	2.7561×10^{-4}	0.9716241	0.116139	0.165796
0.030833	2.2940×10^{-4}	0.9716186	0.117329	0.166137
0.036	1.9645×10^{-4}	0.9716095	0.118747	0.166542
0.041167	1.7175×10^{-4}	0.9715956	0.120397	0.167012
0.046333	1.5254×10^{-4}	0.9715752	0.122287	0.167548
0.0515	1.3717×10^{-4}	0.9715468	0.124423	0.16815
0.056667	1.2458×10^{-4}	0.9715083	0.126812	0.16882
0.061833	1.1407×10^{-4}	0.9714579	0.129463	0.169559
0.067	1.0515×10^{-4}	0.9713931	0.132384	0.170368
0.072167	9.7481×10^{-5}	0.9713115	0.135587	0.171249
0.077333	9.0806×10^{-5}	0.9712105	0.13908	0.172203
0.0825	8.4934×10^{-5}	0.9710874	0.142876	0.173232
0.087667	7.9718×10^{-5}	0.970939	0.146986	0.174338
0.092833	7.5046×10^{-5}	0.9707624	0.151423	0.175523
0.098	7.0827×10^{-5}	0.9705542	0.1562	0.176788
0.10317	6.6990×10^{-5}	0.9703111	0.161329	0.178136
0.10833	6.3476×10^{-5}	0.9700297	0.166826	0.179569
0.1135	6.0238×10^{-5}	0.9697064	0.172704	0.181089
0.11867	5.7236×10^{-5}	0.9693375	0.178977	0.182698

Continued on next page

Table A7-continued from previous page

$\tilde{\alpha}$	β	n_s	r	$\Delta\phi/M_{\rm Pl}$
0.12383	5.4438×10^{-5}	0.9689195	0.185661	0.184399
0.129	5.1817×10^{-5}	0.9684487	0.192769	0.186195
0.13417	4.9349×10^{-5}	0.9679215	0.200317	0.188087
0.13933	4.7016×10^{-5}	0.9673343	0.208318	0.190078
0.1445	4.4801×10^{-5}	0.9666837	0.216787	0.192171
0.14967	4.2690×10^{-5}	0.9659662	0.225736	0.194369
0.15483	4.0673×10^{-5}	0.9651788	0.235178	0.196674
0.16	3.8738×10^{-5}	0.9643184	0.245127	0.199088

Table A8. Semi-analytic, $N_*=80$.

$\tilde{\alpha}$	β	n_s	r	$\Delta\phi/M_{\rm Pl}$
0.005	0.0012391	0.9751537	0.0994859	0.169485
0.010167	6.0941×10^{-4}	0.9751536	0.0997999	0.169589
0.015333	4.0406×10^{-4}	0.975153	0.100329	0.169764
0.0205	3.0221×10^{-4}	0.9751514	0.101076	0.17001
0.025667	2.4136×10^{-4}	0.9751479	0.102044	0.170328
0.030833	2.0089×10^{-4}	0.9751416	0.103237	0.170719
0.036	1.7202×10^{-4}	0.9751312	0.10466	0.171184
0.041167	1.5038×10^{-4}	0.9751153	0.106318	0.171723
0.046333	1.3355×10^{-4}	0.975092	0.10822	0.172337
0.0515	1.2008×10^{-4}	0.9750595	0.110372	0.173029
0.056667	1.0903×10^{-4}	0.9750157	0.112782	0.173799
0.061833	9.9804×10^{-5}	0.9749581	0.115462	0.174649
0.067	9.1971×10^{-5}	0.9748841	0.11842	0.17558
0.072167	8.5226×10^{-5}	0.9747911	0.121668	0.176596
0.077333	7.9347×10^{-5}	0.974676	0.125218	0.177697
0.0825	7.4167×10^{-5}	0.9745356	0.129083	0.178885
0.087667	6.9557×10^{-5}	0.9743666	0.133276	0.180164
0.092833	6.5419×10^{-5}	0.9741656	0.13781	0.181536
0.098	6.1673×10^{-5}	0.9739288	0.142701	0.183002
0.10317	5.8256×10^{-5}	0.9736526	0.147963	0.184567
0.10833	5.5117×10^{-5}	0.9733332	0.153612	0.186232
0.1135	5.2215×10^{-5}	0.9729667	0.159662	0.188
0.11867	4.9516×10^{-5}	0.9725492	0.16613	0.189875
0.12383	4.6990×10^{-5}	0.9720768	0.173032	0.191859
0.129	4.4616×10^{-5}	0.9715457	0.180381	0.193956
0.13417	4.2372×10^{-5}	0.9709522	0.188194	0.196168
0.13933	4.0243×10^{-5}	0.9702926	0.196485	0.198499
0.1445	3.8215×10^{-5}	0.9695634	0.205267	0.200952
0.14967	3.6277×10^{-5}	0.9687615	0.214554	0.203529
0.15483	3.4418×10^{-5}	0.9678839	0.224358	0.206235
0.16	3.2633×10^{-5}	0.9669277	0.234689	0.209072

APPENDIX B: DATA FOR THE MODIFIED KINETIC TERM MODEL

We list the points used to plot Fig. 2 for the modified kinetic-term model, with $M\simeq2.4\times10^{-4}$ fixed. We present both the numerical results and the semi-analytical results obtained using the slow-roll approximation. The first column gives $V_0/10^{-10}$.

Numerical points

Table B1. $\gamma=10$, $n=8$, $N=50$.

V_0	λ	n_s	r	$\Delta\phi/M_{\rm Pl}$	H/M
3	0.021058	0.931357	0.00885	0.86008	0.039266
4.4054	0.022844	0.939657	0.012296	0.78524	0.046366
6.4693	0.019655	0.945116	0.016545	0.7318	0.053901
9.5	0.013541	0.948814	0.021338	0.69741	0.061366

Table B2. $\gamma=10$, $n=8$, $N=60$.

V_0	λ	n_s	r	$\Delta\phi/M_{\rm Pl}$	H/M
3	0.0029811	0.946125	0.0086741	1.0745	0.038866
4.4054	0.0028968	0.951631	0.011898	0.99107	0.045594
6.4693	0.0022291	0.955733	0.015724	0.93438	0.052517
9.5	0.0013993	0.958068	0.019852	0.90065	0.059134

Table B3. $\gamma=10$, $n=8$, $N=70$.

V_0	λ	n_s	r	$\Delta\phi/M_{\rm Pl}$	H/M
3	5.4643e-04	0.955908	0.0084912	1.3017	0.038447
4.4054	4.8253e-04	0.96018	0.011498	1.2118	0.044807
6.4693	3.3948e-04	0.963017	0.014941	1.1539	0.051166
9.5	1.9931e-04	0.964599	0.018516	1.1223	0.057064

Table B4. $\gamma=10$, $n=8$, $N=80$.

V_0	λ	n_s	r	$\Delta\phi/M_{\rm Pl}$	H/M
3	1.2157e-04	0.962842	0.008304	1.5414	0.038016
4.4054	9.8823e-05	0.966155	0.011103	1.4471	0.044019
6.4693	6.4710e-05	0.968161	0.014204	1.3897	0.049867
9.5	3.6206e-05	0.96934	0.017323	1.3613	0.055157

Table B5. $\gamma=10$, $n=10$, $N=50$.

V_0	λ	n_s	r	$\Delta\phi/M_{\rm Pl}$	H/M
3	8.8905e-04	0.934014	0.0088094	0.84912	0.039174
4.4054	9.1425e-04	0.941325	0.012216	0.77667	0.046213
6.4693	7.0744e-04	0.94595	0.016402	0.72503	0.053664
9.5	4.1845e-04	0.949302	0.021113	0.69187	0.061033

Table B6. $\gamma = 10$, $n = 10$, $N = 60$.

V_0	λ	n_s	r	$\Delta\phi/M_{\rm Pl}$	H/M
3	7.4569e-05	0.947793	0.0086269	1.0613	0.038758
4.4054	6.6943e-05	0.952748	0.011808	0.98063	0.045419
6.4693	4.5223e-05	0.956414	0.015572	0.92599	0.052258
9.5	2.3939e-05	0.958596	0.019627	0.89353	0.058791

Table B7. $\gamma = 10$, $n = 10$, $N = 70$.

V_0	λ	n_s	r	$\Delta\phi/M_{\rm Pl}$	H/M
3	8.6873e-06	0.957014	0.008438	1.2861	0.038325
4.4054	6.9357e-06	0.960904	0.011401	1.1994	0.044616
6.4693	4.2054e-06	0.963614	0.014785	1.1437	0.050895
9.5	2.0568e-06	0.964989	0.018297	1.1134	0.056719

Table B8. $\gamma = 10$, $n = 10$, $N = 80$.

V_0	λ	n_s	r	$\Delta\phi/M_{\rm Pl}$	H/M
3	1.2949e-06	0.963727	0.0082458	1.5235	0.037881
4.4054	9.3463e-07	0.966678	0.011001	1.4327	0.043814
6.4693	5.2008e-07	0.968495	0.014048	1.3775	0.049587
9.5	2.4039e-07	0.969618	0.017113	1.3504	0.054816

Table B9. $\gamma = 10$, $n = 12$, $N = 50$.

V_0	λ	n_s	r	$\Delta\phi/M_{\rm Pl}$	H/M
3	2.5050e-05	0.934897	0.0087823	0.8422	0.039113
4.4054	2.4429e-05	0.941484	0.012164	0.77123	0.046111
6.4693	1.7004e-05	0.946355	0.016308	0.72073	0.053507
9.5	8.6395e-06	0.949571	0.020965	0.68833	0.060815

Table B10. $\gamma = 10$, $n = 12$, $N = 60$.

V_0	λ	n_s	r	$\Delta\phi/M_{\rm Pl}$	H/M
3	1.2448e-06	0.948747	0.0085953	1.0529	0.038687
4.4054	1.0328e-06	0.953546	0.011749	0.974	0.045304
6.4693	6.1281e-07	0.956873	0.015473	0.92062	0.052088
9.5	2.7370e-07	0.958941	0.019481	0.88895	0.058566

Table B11. $\gamma = 10$, $n = 12$, $N = 70$.

V_0	λ	n_s	r	$\Delta\phi/M_{\rm Pl}$	H/M
3	9.2173e-08	0.957822	0.0084027	1.2763	0.038244
4.4054	6.6566e-08	0.961552	0.011337	1.1916	0.044489
6.4693	3.4807e-08	0.963913	0.014683	1.1372	0.050716
9.5	1.4186e-08	0.965165	0.018155	1.1076	0.056494

Table B12. $\gamma = 10$, $n = 12$, $N = 80$.

V_0	λ	n_s	r	$\Delta\phi/M_{\rm Pl}$	H/M
3	9.2072e-09	0.9643	0.0082073	1.5121	0.037791
4.4054	5.9035e-09	0.967135	0.010934	1.4235	0.043679
6.4693	2.7932e-09	0.968944	0.013945	1.3697	0.049404
9.5	1.0669e-09	0.969715	0.016976	1.3434	0.054592

Table B13. $\gamma = 12$, $n = 8$, $N = 50$.

V_0	λ	n_s	r	$\Delta\phi/M_{\rm Pl}$	H/M
4.4054	0.022031	0.941187	0.012081	0.77398	0.046002
6.4693	0.018215	0.946138	0.016098	0.72329	0.053229
9.5	0.012089	0.949198	0.020514	0.69164	0.060249

Table B14. $\gamma = 12$, $n = 8$, $N = 60$.

V_0	λ	n_s	r	$\Delta\phi/M_{\rm Pl}$	H/M
4.4054	0.0026752	0.952769	0.011645	0.98111	0.045145
6.4693	0.001977	0.95638	0.015222	0.92797	0.051725
9.5	0.0012012	0.958461	0.018981	0.89748	0.057889

Table B15. $\gamma = 12$, $n = 8$, $N = 70$.

V_0	λ	n_s	r	$\Delta\phi/M_{\rm Pl}$	H/M
4.4054	4.2921e-04	0.960895	0.011211	1.2043	0.04428
6.4693	2.9049e-04	0.963483	0.014398	1.1507	0.050275
9.5	1.6597e-04	0.964898	0.017622	1.1228	0.055726

Table B16. $\gamma = 12$, $n = 8$, $N = 80$.

V_0	λ	n_s	r	$\Delta\phi/M_{\rm Pl}$	H/M
4.4054	8.5089e-05	0.966759	0.010787	1.4432	0.04342
6.4693	5.3764e-05	0.968638	0.013632	1.3907	0.048893
9.5	2.9423e-05	0.969549	0.016424	1.3664	0.053755

Table B17. $\gamma = 12$, $n = 10$, $N = 50$.

V_0	λ	n_s	r	$\Delta\phi/M_{\rm Pl}$	H/M
4.4054	8.5905e-04	0.941387	0.011997	0.76592	0.045838
6.4693	6.3342e-04	0.946882	0.015951	0.71693	0.052981
9.5	3.5844e-04	0.949956	0.020291	0.68639	0.059912

Table B18. $\gamma = 12$, $n = 10$, $N = 60$.

V_0	λ	n_s	r	$\Delta\phi/M_{\rm Pl}$	H/M
4.4054	5.9614e-05	0.953875	0.011552	0.97127	0.044961
6.4693	3.8370e-05	0.95705	0.015069	0.92001	0.051459
9.5	1.9553e-05	0.959008	0.018762	0.89064	0.057546

Table B19. $\gamma = 12$, $n = 10$, $N = 70$.

V_0	λ	n_s	r	$\Delta\phi/M_{\rm Pl}$	H/M
4.4054	5.8977e-06	0.961737	0.011111	1.1926	0.044079
6.4693	3.4157e-06	0.964046	0.014243	1.141	0.049998
9.5	1.6188e-06	0.965173	0.017412	1.1141	0.055385

Table B20. $\gamma = 12$, $n = 10$, $N = 80$.

V_0	λ	n_s	r	$\Delta\phi/M_{\rm Pl}$	H/M
4.4054	7.6373e-07	0.96733	0.010683	1.4295	0.043207
6.4693	4.0751e-07	0.968998	0.013478	1.379	0.048611
9.5	1.8366e-07	0.969752	0.016223	1.3557	0.053419

Table B21. $\gamma = 12$, $n = 12$, $N = 50$.

V_0	λ	n_s	r	$\Delta\phi/M_{\rm Pl}$	H/M
4.4054	2.2365e-05	0.943329	0.011942	0.76081	0.04573
6.4693	1.4711e-05	0.947593	0.015855	0.71288	0.052818
9.5	7.1038e-06	0.950279	0.020146	0.68301	0.059691

Table B22. $\gamma = 12$, $n = 12$, $N = 60$.

V_0	λ	n_s	r	$\Delta\phi/M_{\rm Pl}$	H/M
4.4054	8.8700e-07	0.954471	0.01149	0.96501	0.044839
6.4693	4.9751e-07	0.957372	0.014969	0.91492	0.051284
9.5	2.1271e-07	0.959237	0.018619	0.88624	0.057321

Table B23. $\gamma = 12$, $n = 12$, $N = 70$.

V_0	λ	n_s	r	$\Delta\phi/M_{\rm Pl}$	H/M
4.4054	5.4120e-08	0.962185	0.011046	1.1851	0.043947
6.4693	2.6836e-08	0.964363	0.014141	1.1347	0.049816
9.5	1.0553e-08	0.965515	0.017275	1.1085	0.055162

Table B24. $\gamma = 12$, $n = 12$, $N = 80$.

V_0	λ	n_s	r	$\Delta\phi/M_{\rm Pl}$	H/M
4.4054	4.5786e-09	0.967677	0.010615	1.4207	0.043067
6.4693	2.0642e-09	0.969228	0.013377	1.3715	0.048427
9.5	7.6631e-10	0.96994	0.016093	1.3488	0.0532

Semi-analytic Points

Table B25. $\gamma = 10$, $n = 8$, $N = 50$.

V_0	λ	n_s	r	$\Delta\phi/M_{\rm Pl}$	H/M
3	0.01925	0.932736	0.0089542	0.80419	0.039318
4.4054	0.020452	0.940342	0.012489	0.73196	0.046435
6.4693	0.017132	0.946055	0.016874	0.68002	0.053974
9.5	0.011444	0.949799	0.021845	0.6461	0.061412
13.951	0.0064393	0.951838	0.026949	0.62671	0.06821
20.486	0.0032937	0.952659	0.03176	0.61766	0.074049
30.083	0.0016348	0.952744	0.036043	0.6152	0.078884
44.177	8.2016e-04	0.952439	0.03974	0.61659	0.082831
64.873	4.2440e-04	0.951949	0.042896	0.62012	0.086057
95.264	2.2824e-04	0.951388	0.045587	0.62477	0.088716

Table B26. $\gamma = 10$, $n = 8$, $N = 60$.

V_0	λ	n_s	r	$\Delta\phi/M_{\rm Pl}$	H/M
1.3912	0.0015532	0.931666	0.0043408	1.2526	0.027332
2.0429	0.0022738	0.939867	0.0062101	1.1137	0.032744
3	0.0027195	0.946964	0.0087692	1.0051	0.03891
4.4054	0.0025896	0.952599	0.012068	0.92416	0.045645
6.4693	0.001944	0.956591	0.016001	0.86856	0.052559
9.5	0.0011884	0.959007	0.020257	0.83461	0.059137
13.951	6.3388e-04	0.960179	0.024444	0.81713	0.064962
20.486	3.1773e-04	0.960532	0.028272	0.81072	0.069864
30.083	1.5800e-04	0.960421	0.031622	0.81103	0.073887
44.177	8.0330e-05	0.960076	0.034493	0.81517	0.07717
64.873	4.2321e-05	0.95963	0.036942	0.82134	0.079861
95.264	2.3196e-05	0.959151	0.039034	0.8285	0.082092

Table B27. $\gamma = 10$, $n = 8$, $N = 70$.

V_0	λ	n_s	r	$\Delta\phi/M_{\rm Pl}$	H/M
0.94737	2.0968e-04	0.936586	0.0029736	1.6935	0.022658
1.3912	3.3630e-04	0.944185	0.0042944	1.4969	0.027229
2.0429	4.5449e-04	0.950917	0.0061291	1.3393	0.032529
3	4.9834e-04	0.956539	0.0085781	1.218	0.038483
4.4054	4.3160e-04	0.960826	0.011648	1.1303	0.044844
6.4693	2.9685e-04	0.963695	0.015175	1.0729	0.051185
9.5	1.7039e-04	0.965302	0.018845	1.0402	0.05704
13.951	8.7993e-05	0.965986	0.02234	1.0254	0.062105
20.486	4.3761e-05	0.9661	0.025471	1.0221	0.066313
30.083	2.1906e-05	0.965906	0.028182	1.0256	0.069753
44.177	1.1288e-05	0.965565	0.030498	1.0328	0.072563
64.873	6.0414e-06	0.965165	0.032473	1.0419	0.074876
95.264	3.3643e-06	0.964752	0.034165	1.0519	0.076801

Table B28. $\gamma = 10$, $n = 8$, $N = 80$.

V_0	λ	n_s	r	$\Delta\phi/M_{\rm Pl}$	H/M
0.94737	5.7087e-05	0.946803	0.0029595	1.9718	0.022604
1.3912	8.6703e-05	0.95322	0.0042596	1.7503	0.027118
2.0429	1.0951e-04	0.958808	0.0060449	1.5749	0.032305
3	1.1095e-04	0.96335	0.0083837	1.4426	0.038045
4.4054	8.8532e-05	0.966677	0.011236	1.35	0.044044
6.4693	5.6805e-05	0.968784	0.014404	1.2923	0.049868
9.5	3.1177e-05	0.969876	0.017595	1.2619	0.055115
13.951	1.5793e-05	0.970271	0.02056	1.2504	0.059579
20.486	7.8444e-06	0.970257	0.023178	1.2507	0.063258
30.083	3.9602e-06	0.97003	0.025431	1.2576	0.066261
44.177	2.0668e-06	0.969707	0.027352	1.2682	0.068719
64.873	1.1216e-06	0.969348	0.028993	1.2805	0.07075
95.264	6.3307e-07	0.968987	0.030401	1.2935	0.072447

Table B29. $\gamma = 10$, $n = 10$, $N = 50$.

V_0	λ	n_s	r	$\Delta\phi/M_{\rm Pl}$	H/M
3	7.9674e-04	0.934977	0.0089122	0.79573	0.039226
4.4054	7.9793e-04	0.941878	0.012406	0.72549	0.04628
6.4693	5.9685e-04	0.947069	0.016724	0.67507	0.053734
9.5	3.3975e-04	0.950468	0.021607	0.64215	0.061077
13.951	1.5785e-04	0.952304	0.026622	0.62331	0.067795
20.486	6.5702e-05	0.953019	0.03136	0.61451	0.073581
30.083	2.6505e-05	0.953051	0.035593	0.61212	0.07839
44.177	1.0882e-05	0.952717	0.039263	0.61352	0.082332
64.873	4.6575e-06	0.95221	0.042408	0.61703	0.085566
95.264	2.0963e-06	0.951638	0.045099	0.62167	0.08824

Table B30. $\gamma = 10$, $n = 10$, $N = 60$.

V_0	λ	n_s	r	$\Delta\phi/M_{\rm Pl}$	H/M
1.3912	3.8760e-05	0.934667	0.0043165	1.2351	0.027299
2.0429	5.7397e-05	0.942118	0.0061864	1.1004	0.032681
3	6.6599e-05	0.948543	0.0087204	0.99484	0.038801
4.4054	5.8276e-05	0.953661	0.011975	0.91628	0.045469
6.4693	3.8168e-05	0.957287	0.015843	0.86238	0.052299
9.5	1.9553e-05	0.959476	0.020022	0.82948	0.058794
13.951	8.5371e-06	0.960521	0.024139	0.81252	0.064556
20.486	3.4762e-06	0.960809	0.027915	0.8063	0.069422
30.083	1.4087e-06	0.960665	0.031233	0.80667	0.073432
44.177	5.8895e-07	0.960302	0.034089	0.8108	0.076716
64.873	2.5807e-07	0.959844	0.036533	0.81695	0.079418
95.264	1.1905e-07	0.959356	0.038627	0.8241	0.081663

Table B31. $\gamma = 10$, $n = 10$, $N = 70$.

V_0	λ	n_s	r	$\Delta\phi/M_{\rm Pl}$	H/M
0.94737	3.2803e-06	0.939715	0.0029677	1.6683	0.022635
1.3912	5.5055e-06	0.946529	0.0042815	1.4769	0.027188
2.0429	7.4438e-06	0.952606	0.0061017	1.3237	0.032457
3	7.7525e-06	0.957704	0.0085234	1.2059	0.038361
4.4054	6.0397e-06	0.961598	0.011548	1.1209	0.044651
6.4693	3.5608e-06	0.964203	0.015014	1.0653	0.050912
9.5	1.6935e-06	0.965654	0.018618	1.0337	0.056695
13.951	7.1265e-07	0.966254	0.022059	1.0194	0.061712
20.486	2.8802e-07	0.966325	0.025151	1.0163	0.065896
30.083	1.1787e-07	0.966109	0.027841	1.0198	0.06933
44.177	5.0167e-08	0.965755	0.030148	1.027	0.072145
64.873	2.2439e-08	0.965346	0.032122	1.0361	0.07447
95.264	1.0566e-08	0.964926	0.033818	1.046	0.07641

Table B32. $\gamma = 10$, $n = 10$, $N = 80$.

V_0	λ	n_s	r	$\Delta\phi/M_{\rm Pl}$	H/M
0.94737	6.2922e-07	0.949296	0.0029527	1.9427	0.022578
1.3912	9.8565e-07	0.955066	0.0042448	1.7273	0.027071
2.0429	1.2406e-06	0.960081	0.0059978	1.556	0.032229
3	1.1563e-06	0.96424	0.008324	1.4286	0.037909
4.4054	8.1544e-07	0.967262	0.011131	1.339	0.043837
6.4693	4.4246e-07	0.969173	0.014243	1.2832	0.049588
9.5	1.9970e-07	0.970153	0.017378	1.2538	0.054774
13.951	8.2253e-08	0.97049	0.0203	1.2428	0.0592
20.486	3.3248e-08	0.970446	0.02289	1.2432	0.062864
30.083	1.3768e-08	0.970204	0.025128	1.2502	0.065865
44.177	5.9587e-09	0.96987	0.027044	1.2607	0.068331
64.873	2.7135e-09	0.969505	0.028685	1.273	0.070374
95.264	1.3004e-09	0.969138	0.030098	1.286	0.072086

Table B33. $\gamma = 10$, $n = 12$, $N = 50$.

V_0	λ	n_s	r	$\Delta\phi/M_{\rm Pl}$	H/M
3	2.2004e-05	0.936355	0.0088841	0.7904	0.039164
4.4054	2.0779e-05	0.94283	0.012351	0.72141	0.046177
6.4693	1.3887e-05	0.947705	0.016626	0.67192	0.053575
9.5	6.7397e-06	0.950893	0.021453	0.63962	0.060858
13.951	2.5863e-06	0.952605	0.026409	0.62113	0.067523
20.486	8.7615e-07	0.953254	0.031099	0.61247	0.073275
30.083	2.8730e-07	0.953251	0.0353	0.61012	0.078067
44.177	9.6531e-08	0.952899	0.038952	0.61152	0.082006
64.873	3.4170e-08	0.952382	0.04209	0.61502	0.085244
95.264	1.2871e-08	0.951802	0.04478	0.61965	0.087927

Table B34. $\gamma = 10$, $n = 12$, $N = 60$.

V_0	λ	n_s	r	$\Delta\phi/M_{\rm Pl}$	H/M
1.3912	6.4068e-07	0.936534	0.004309	1.2245	0.027275
2.0429	9.6686e-07	0.943496	0.0061704	1.0921	0.032639
3	1.0884e-06	0.949518	0.0086879	0.98836	0.038729
4.4054	8.7555e-07	0.954322	0.011914	0.91128	0.045353
6.4693	5.0059e-07	0.957727	0.015739	0.85844	0.052128
9.5	2.1499e-07	0.959775	0.01987	0.82618	0.05857
13.951	7.6859e-08	0.960742	0.023941	0.80954	0.064291
20.486	2.5426e-08	0.960989	0.027683	0.80345	0.069133
30.083	8.3969e-09	0.960824	0.03098	0.80384	0.073134
44.177	2.8868e-09	0.96045	0.033825	0.80795	0.076418
64.873	1.0521e-09	0.959984	0.036266	0.81409	0.079127
95.264	4.0823e-10	0.959491	0.038362	0.82127	0.081379

Table B35. $\gamma = 10$, $n = 12$, $N = 70$.

V_0	λ	n_s	r	$\Delta\phi/M_{\rm Pl}$	H/M
0.94737	3.4263e-08	0.941607	0.0029636	1.6525	0.02262
1.3912	6.0151e-08	0.947958	0.0042727	1.4643	0.02716
2.0429	8.1354e-08	0.953644	0.0060835	1.3139	0.032408
3	8.0494e-08	0.958425	0.0084871	1.1982	0.038279
4.4054	5.6441e-08	0.962082	0.011482	1.115	0.044524
6.4693	2.8538e-08	0.964526	0.014908	1.0605	0.050733
9.5	1.1250e-08	0.96588	0.018471	1.0295	0.05647
13.951	3.8583e-09	0.966427	0.021875	1.0155	0.061455
20.486	1.2673e-09	0.966472	0.024943	1.0125	0.065623
30.083	4.2390e-10	0.966242	0.027619	1.016	0.069052
44.177	1.4919e-10	0.96588	0.029919	1.0231	0.071874
64.873	5.5762e-11	0.965465	0.031892	1.0322	0.074206
95.264	2.2096e-11	0.96504	0.033592	1.0424	0.076135

Table B36. $\gamma = 10$, $n = 12$, $N = 80$.

V_0	λ	n_s	r	$\Delta\phi/M_{\rm Pl}$	H/M
0.94737	4.6299e-09	0.950808	0.002948	1.9244	0.02256
1.3912	7.4774e-09	0.956193	0.0042349	1.7128	0.02704
2.0429	9.1341e-09	0.960925	0.0059938	1.5456	0.032168
3	8.0442e-09	0.964793	0.0082845	1.4198	0.037819
4.4054	5.0165e-09	0.967631	0.011062	1.3321	0.043702
6.4693	2.3031e-09	0.969421	0.014137	1.2774	0.049404
9.5	8.5513e-10	0.970332	0.017237	1.2486	0.054551
13.951	2.8642e-10	0.970633	0.020131	1.2379	0.058953
20.486	9.4220e-11	0.97057	0.022702	1.2383	0.062606
30.083	3.2168e-11	0.970318	0.024927	1.2449	0.065623
44.177	1.1617e-11	0.969979	0.026836	1.255	0.068117
64.873	4.2595e-12	0.969604	0.0285	1.2704	0.070011
95.264	1.7380e-12	0.969234	0.029912	1.2833	0.071735

Table B37. $\gamma = 12$, $n = 8$, $N = 50$.

V_0	λ	n_s	r	$\Delta\phi/M_{\rm Pl}$	H/M
3	0.019089	0.934389	0.0088714	0.79046	0.039136
4.4054	0.019586	0.941743	0.012294	0.72042	0.04607
6.4693	0.015732	0.947094	0.016452	0.67109	0.053295
9.5	0.01	0.950469	0.021074	0.64025	0.060251
13.951	0.0055502	0.952183	0.025646	0.62238	0.06654
20.486	0.0028107	0.952802	0.029896	0.61469	0.071843
30.083	0.0013963	0.952778	0.033631	0.61298	0.076199
44.177	7.0535e-04	0.952423	0.036835	0.61473	0.079746
64.873	3.6841e-04	0.951919	0.039562	0.61837	0.082645
95.264	2.0010e-04	0.951361	0.041886	0.623	0.085037

Table B38. $\gamma = 12$, $n = 8$, $N = 60$.

V_0	λ	n_s	r	$\Delta\phi/M_{\rm Pl}$	H/M
1.3912	0.0015601	0.933054	0.0043107	1.2353	0.02728
2.0429	0.0022312	0.94131	0.0061674	1.098	0.032631
3	0.0025937	0.948262	0.0086649	0.99148	0.038678
4.4054	0.0023748	0.953636	0.01183	0.91351	0.045194
6.4693	0.0017099	0.957306	0.015517	0.86124	0.051758
9.5	0.0010114	0.959423	0.019403	0.83029	0.057877
13.951	5.3000e-04	0.960377	0.023137	0.81501	0.063202
20.486	2.6454e-04	0.960601	0.026496	0.80996	0.067635
30.083	1.3210e-04	0.960425	0.029407	0.81098	0.071254
44.177	6.7725e-05	0.960055	0.031892	0.81541	0.074202
64.873	3.6030e-05	0.959605	0.034006	0.82163	0.076622
95.264	1.9942e-05	0.959133	0.035812	0.82872	0.078631

Table B39. $\gamma = 12$, $n = 8$, $N = 70$.

V_0	λ	n_s	r	$\Delta\phi/M_{\rm Pl}$	H/M
0.94737	2.0556e-04	0.9378	0.0029653	1.6768	0.022626
1.3912	3.2691e-04	0.945445	0.0042733	1.48	0.027162
2.0429	4.3277e-04	0.952119	0.0060765	1.324	0.03239
3	4.5898e-04	0.957574	0.0084527	1.2054	0.038201
4.4054	3.8133e-04	0.961609	0.011373	1.1216	0.044312
6.4693	2.5213e-04	0.964201	0.014645	1.0681	0.050283
9.5	1.4084e-04	0.965576	0.017963	1.0388	0.055688
13.951	7.1871e-05	0.966105	0.021058	1.0263	0.060295
20.486	3.5733e-05	0.966132	0.023792	1.0244	0.064091
30.083	1.7999e-05	0.965899	0.026143	1.0285	0.067182
44.177	9.3601e-06	0.965545	0.028144	1.036	0.069707
64.873	5.0593e-06	0.965146	0.02985	1.0451	0.071787
95.264	2.8447e-06	0.96474	0.03131	1.0549	0.073523

Table B40. $\gamma = 12$, $n = 8$, $N = 80$.

V_0	λ	n_s	r	$\Delta\phi/M_{\rm Pl}$	H/M
0.94737	5.4894e-05	0.947891	0.0029495	1.9555	0.022566
1.3912	8.2342e-05	0.954319	0.0042342	1.7341	0.027037
2.0429	1.0142e-04	0.959822	0.0059823	1.5608	0.032138
3	9.9022e-05	0.964188	0.0082381	1.4322	0.037713
4.4054	7.5754e-05	0.967279	0.010929	1.3442	0.043439
6.4693	4.6880e-05	0.969151	0.013842	1.2911	0.048885
9.5	2.5174e-05	0.970061	0.016703	1.2643	0.0537
13.951	1.2659e-05	0.970343	0.019314	1.2552	0.057745
20.486	6.3035e-06	0.97027	0.021594	1.2567	0.061058
30.083	3.2064e-06	0.970018	0.023544	1.2643	0.063756
44.177	1.6894e-06	0.969688	0.025204	1.275	0.065965
64.873	9.2588e-07	0.969333	0.02662	1.2873	0.067793
95.264	5.2758e-07	0.96898	0.027836	1.3002	0.069324

Table B41. $\gamma = 12$, $n = 10$, $N = 50$.

V_0	λ	n_s	r	$\Delta\phi/M_{\rm Pl}$	H/M
3	7.7458e-04	0.936462	0.0088263	0.78256	0.039036
4.4054	7.4310e-04	0.943141	0.012206	0.71443	0.045905
6.4693	5.2838e-04	0.948006	0.016298	0.66651	0.053045
9.5	2.8745e-04	0.951058	0.020811	0.63603	0.059941
13.951	1.2975e-04	0.952611	0.025331	0.61915	0.066131
20.486	5.3435e-05	0.953141	0.029521	0.61164	0.071391
30.083	2.1607e-05	0.953071	0.033218	0.60997	0.07573
44.177	8.9550e-06	0.952692	0.036403	0.61172	0.079277
64.873	3.8799e-06	0.952172	0.039123	0.61535	0.082185
95.264	1.7689e-06	0.951604	0.041449	0.61995	0.084593

Table B42. $\gamma = 12$, $n = 10$, $N = 60$.

V_0	λ	n_s	r	$\Delta\phi/M_{\rm Pl}$	H/M
1.3912	3.7948e-05	0.935961	0.0042986	1.2192	0.027242
2.0429	5.5082e-05	0.943409	0.0061416	1.0855	0.032563
3	6.1679e-05	0.949711	0.0086128	0.98189	0.038561
4.4054	5.1446e-05	0.954596	0.011733	0.90617	0.045008
6.4693	3.2054e-05	0.957932	0.015357	0.85546	0.051491
9.5	1.5801e-05	0.959849	0.019173	0.82542	0.057534
13.951	6.7624e-06	0.960695	0.022848	0.81056	0.062806
20.486	2.7432e-06	0.960864	0.026165	0.80565	0.067211
30.083	1.1186e-06	0.96066	0.029052	0.8067	0.070822
44.177	4.7291e-07	0.960274	0.031526	0.81111	0.073776
64.873	2.0987e-07	0.959813	0.033639	0.81731	0.076208
95.264	9.8054e-08	0.959333	0.035449	0.82439	0.078231

Table B43. $\gamma = 12$, $n = 10$, $N = 70$.

V_0	λ	n_s	r	$\Delta\phi/M_{\rm Pl}$	H/M
0.94737	3.1470e-06	0.940783	0.0029589	1.6527	0.022602
1.3912	5.2229e-06	0.947652	0.0042593	1.4611	0.027117
2.0429	6.8792e-06	0.953685	0.006047	1.3092	0.032311
3	6.8751e-06	0.958637	0.0083947	1.1941	0.03807
4.4054	5.0934e-06	0.962305	0.01127	1.1128	0.04411
6.4693	2.8655e-06	0.964659	0.014484	1.061	0.050006
9.5	1.3207e-06	0.965898	0.017744	1.0326	0.055348
13.951	5.4861e-07	0.966355	0.020793	1.0205	0.059915
20.486	2.2193e-07	0.966347	0.023498	1.0186	0.063693
30.083	9.1613e-08	0.966095	0.025833	1.0228	0.066783
44.177	3.9464e-08	0.965729	0.027829	1.0302	0.069315
64.873	1.7880e-08	0.965322	0.029535	1.0393	0.071408
95.264	8.5250e-09	0.96491	0.031	1.0491	0.073158

Table B44. $\gamma = 12$, $n = 10$, $N = 80$.

V_0	λ	n_s	r	$\Delta\phi/M_{\rm Pl}$	H/M
0.94737	5.8912e-07	0.950257	0.002942	1.9277	0.022537
1.3912	9.0807e-07	0.956046	0.0042182	1.7123	0.026986
2.0429	1.0929e-06	0.96103	0.0059494	1.5439	0.032049
3	9.8632e-07	0.964996	0.0081753	1.4191	0.037569
4.4054	6.6119e-07	0.967806	0.010822	1.3339	0.043225
6.4693	3.4383e-07	0.969503	0.013682	1.2825	0.048602
9.5	1.5137e-07	0.970317	0.016496	1.2565	0.053366
13.951	6.1880e-08	0.97055	0.019072	1.2477	0.057382
20.486	2.5119e-08	0.970451	0.02133	1.2493	0.060684
30.083	1.0508e-08	0.970186	0.02327	1.2569	0.063384
44.177	4.6052e-09	0.969847	0.024927	1.2676	0.065602
64.873	2.1242e-09	0.969486	0.026345	1.2799	0.067442
95.264	1.0304e-09	0.969128	0.027566	1.2927	0.068987

Table B45. $\gamma = 12$, $n = 12$, $N = 50$.

V_0	λ	n_s	r	$\Delta\phi/M_{\rm Pl}$	H/M
2.0429	1.6707e-05	0.930024	0.0062176	0.86633	0.032764
3	2.0974e-05	0.937739	0.0087962	0.77758	0.03897
4.4054	1.8820e-05	0.94401	0.012148	0.71064	0.045795
6.4693	1.1852e-05	0.948581	0.016197	0.66359	0.05288
9.5	5.4593e-06	0.951443	0.020657	0.63367	0.059719
13.951	2.0276e-06	0.952888	0.025126	0.61707	0.065863
20.486	6.7913e-07	0.953361	0.029277	0.60966	0.071095
30.083	2.2354e-07	0.953263	0.032949	0.60803	0.075423
44.177	7.6008e-08	0.952868	0.036121	0.60976	0.078969
64.873	2.7317e-08	0.952339	0.038836	0.61338	0.081884
95.264	1.0454e-08	0.951764	0.041163	0.61797	0.084301

Table B46. $\gamma = 12$, $n = 12$, $N = 60$.

V_0	λ	n_s	r	$\Delta\phi/M_{\rm Pl}$	H/M
1.3912	6.1609e-07	0.93773	0.0042904	1.2091	0.027216
2.0429	9.0736e-07	0.944696	0.0061244	1.0776	0.032517
3	9.7890e-07	0.950608	0.0085781	0.97584	0.038484
4.4054	7.4414e-07	0.955196	0.01167	0.90152	0.044885
6.4693	4.0145e-07	0.958329	0.015252	0.85177	0.051315
9.5	1.6498e-07	0.960122	0.019024	0.82229	0.05731
13.951	5.7680e-08	0.9609	0.02266	0.80769	0.062548
20.486	1.9017e-08	0.961035	0.02595	0.80286	0.066934
30.083	6.3329e-09	0.960814	0.028821	0.80392	0.07054
44.177	2.2076e-09	0.960418	0.031288	0.80831	0.073496
64.873	8.1718e-10	0.95995	0.033399	0.81451	0.075935
95.264	3.2250e-10	0.959465	0.035211	0.82154	0.077971

Table B47. $\gamma = 12$, $n = 12$, $N = 70$.

V_0	λ	n_s	r	$\Delta\phi/M_{\rm Pl}$	H/M
0.94737	3.2162e-08	0.942589	0.0029545	1.6376	0.022585
1.3912	5.5684e-08	0.948998	0.0042498	1.4492	0.027087
2.0429	7.2968e-08	0.954649	0.0060274	1.3	0.032258
3	6.8741e-08	0.959297	0.0083563	1.187	0.037983
4.4054	4.5436e-08	0.962743	0.011202	1.1072	0.043977
6.4693	2.1762e-08	0.964951	0.014379	1.0565	0.049824
9.5	8.2783e-09	0.966105	0.017601	1.0286	0.055125
13.951	2.7995e-09	0.966518	0.020621	1.0167	0.059667
20.486	9.2145e-10	0.966488	0.023306	1.0149	0.063433
30.083	3.1156e-10	0.966223	0.025631	1.0191	0.06652
44.177	1.1134e-10	0.96585	0.027622	1.0264	0.069061
64.873	4.2280e-11	0.965438	0.029329	1.0354	0.071162
95.264	1.6917e-11	0.96502	0.030802	1.0459	0.072878

Table B48. $\gamma = 12$, $n = 12$, $N = 80$.

V_0	λ	n_s	r	$\Delta\phi/M_{\rm Pl}$	H/M
0.94737	4.1521e-09	0.951755	0.0029485	1.9113	0.022516
1.3912	6.6824e-09	0.957103	0.0042075	1.6985	0.026952
2.0429	7.8589e-09	0.961775	0.0059275	1.5332	0.03199
3	6.5589e-09	0.965499	0.0081338	1.4108	0.037474
4.4054	3.8550e-09	0.968138	0.010752	1.3273	0.043085
6.4693	1.6853e-09	0.969728	0.013578	1.2769	0.048418
9.5	6.0845e-10	0.970483	0.016361	1.2515	0.053148
13.951	2.0224e-10	0.970685	0.018914	1.2429	0.057144
20.486	6.6843e-11	0.97057	0.021159	1.2446	0.060436
30.083	2.3159e-11	0.970296	0.023088	1.2517	0.063158
44.177	8.6030e-12	0.969955	0.024734	1.2609	0.065448
64.873	3.1540e-12	0.969582	0.02618	1.2775	0.067092

Table B49. Evolution along the γ branch for $n = 10$, $M = 2.45\times10^{-4}$, $V_0 = 4.4054\times10^{-10}$, $N = 80$.

γ	c_s	λ	n_s	r	$\Delta\phi/M_{\rm Pl}$	H/M
3	0.44721	5.5803e-08	0.964045	0.0125433	2.01119	0.0465355
4	0.37796	2.6650e-07	0.964478	0.0123076	1.67383	0.0460962
5	0.33333	5.4666e-07	0.965061	0.0120806	1.52043	0.0456692
6	0.30151	7.6535e-07	0.96562	0.0118665	1.43894	0.0452627
8	0.2582	9.0768e-07	0.966554	0.0114765	1.36443	0.0445126
10	0.22942	8.1544e-07	0.967262	0.011131	1.33904	0.0438374
12	0.20851	6.6119e-07	0.967806	0.0108222	1.33393	0.0432251
16	0.17961	3.9818e-07	0.968572	0.0102909	1.34831	0.0421507
20	0.16013	2.3905e-07	0.969078	0.00984653	1.375	0.0412306
30	0.13019	7.8288e-08	0.969798	0.00898546	1.45193	0.0393866
40	0.11251	3.1914e-08	0.970164	0.00834899	1.52576	0.037966
50	0.1005	1.5262e-08	0.970375	0.0078503	1.59299	0.0368147

References

[1] A. H. Guth, Phys. Rev. D **23**, 347 (1981)
[2] A. D. Linde, Phys. Lett. B **108**, 389 (1982)
[3] A. Albrecht and P. J. Steinhardt, Phys. Rev. Lett. **48**, 1220 (1982)
[4] A. A. Starobinsky, Phys. Lett. B **91**, 99 (1980)
[5] V. F. Mukhanov and G. V. Chibisov, JETP Lett. **33**, 532 (1981)
[6] D. Baumann, Inflation, in *Physics of the Large and the Small*, edited by C. Csaki and S. Dodelson (Singapore: World Scientific, 2011), p. 523–686
[7] J. Martin, C. Ringeval, and V. Vennin, Phys. Dark Univ. **5-6**, 75 (2014)
[8] D. H. Lyth, Phys. Rev. Lett. **78**, 1861 (1997)
[9] G. Efstathiou and K. J. Mack, JCAP **05**, 008 (2005)
[10] M. Alishahiha, E. Silverstein, and D. Tong, Phys. Rev. D **70**, 123505 (2004)
[11] D. Baumann and L. McAllister, Phys. Rev. D **75**, 123508 (2007)
[12] S. Antusch and D. Nolde, JCAP **05**, 035 (2014)
[13] N. K. Stein and W. H. Kinney, JCAP **04**, 006 (2017)
[14] Y. Akrami *et al.* (Planck Collaboration), Astron. Astrophys. **641**, A10 (2020)
[15] R. Bravo, G. A. Palma and S. Riquelme, JCAP **02**, 004 (2020)
[16] P. A. R. Ade *et al.* (BICEP/Keck Collaboration), Phys. Rev. Lett. **127**(15), 151301 (2021)
[17] Y.-F. Cai, J. Jiang, M. Sasaki *et al.*, Phys. Rev. Lett. **127**(25), 251301 (2021)
[18] D. Paoletti, F. Finelli, J. Valiviita *et al.*, Phys. Rev. D **106**(8), 083528 (2022)
[19] E. Calabrese *et al.* (Atacama Cosmology Telescope Collaboration), JCAP **11**, 063 (2025)
[20] Y. S. Furuta, Y. Hamada, and K. Kohri, Phys. Rev. D **112**(10), 103517 (2025)

[21] S. Akama and C. Lin, arXiv: 2602.20734
[22] W. Xue and B. Chen, Phys. Rev. D **79**, 043518 (2009)
[23] A. Ashoorioon, K. Dimopoulos, M. M. Sheikh-Jabbari *et al*., Phys. Lett. B **737**, 98 (2014)
[24] A. Ashoorioon, K. Dimopoulos, M. M. Sheikh-Jabbari *et al*., JCAP **02**, 025 (2014)
[25] X. Li, S. Wang, and Z. Chang, Eur. Phys. J. C **75**(6), 260 (2015)
[26] X. Zhang and Y. Ling, JCAP **08**, 012 (2007)
[27] J. Hartong, A. Ploegh, T. Van Riet *et al*., Class. Quant. Grav. **23**, 4593 (2006)
[28] B. M. Gu, F. W. Shu, and K. Yang, Phys. Dark Univ. **47**, 101744 (2025)
[29] B. M. Gu, Y. P. Zhang, F. W. Shu *et al*., arXiv: 2602.07972
[30] H. Zhang and L. Xu, JCAP **10**, 003 (2020)
[31] T. C. Li, T. Zhu, W. Zhao *et al*., JCAP **07**, 005 (2024)
[32] Q. G. Huang, Phys. Rev. D **91**(12), 123532 (2015)
[33] N. Aghanim *et al*. (Planck Collaboration), Astron. Astrophys. **641**, A6 (2020)
[34] R. Easther, W. H. Kinney, and B. A. Powell, JCAP **08**, 004 (2006)
[35] J. Garcia-Bellido, D. Roest, M. Scalisi *et al*., JCAP **09**, 006 (2014)
[36] J. Garcia-Bellido, D. Roest, M. Scalisi *et al*., Phys. Rev. D **90**(12), 123539 (2014)
[37] T. Louis *et al*. (Atacama Cosmology Telescope Collaboration), JCAP **11**, 062 (2025)
[38] R. Kallosh, A. Linde, and D. Roest, Phys. Rev. Lett. **135**(16), 161001 (2025)
[39] C. Dioguardi, A. J. Iovino, and A. Racioppi, Phys. Lett. B **868**, 139664 (2025)
[40] E. G. M. Ferreira, E. McDonough, L. Balkenhol *et al*., Phys. Rev. D **113**(4), 043524 (2026)
[41] E. McDonough and E. G. M. Ferreira, arXiv: 2512.05108
[42] Y. Zhu, Q. Gao, Y. Gong *et al*., Eur. Phys. J. C **85**(10), 1227 (2025)
[43] Q. Gao, Y. Qian, Y. Gong *et al*., JCAP **08**, 083 (2025)
[44] Z. Yi, X. Wang, Q. Gao *et al*., Phys. Lett. B **871**, 140002 (2025)
[45] M. He, M. Hong, and K. Mukaida, JCAP **09**, 080 (2025)
[46] F. J. Qu *et al*. (ACT Collaboration), Astrophys. J. **962**(2), 112 (2024)
[47] Y. H. Pang, X. Zhang, and Q. G. Huang, Phys. Rev. D **111**(12), 123504 (2025)
[48] Q. Gao, Y. Gong, Z. Yi *et al*., Phys. Dark Univ. **50**, 102106 (2025)
[49] L. Liu, Z. Yi, and Y. Gong, arXiv: 2505.02407
[50] Z. Z. Peng, Z. C. Chen, and L. Liu, Phys. Rev. D **113**(6), 063527 (2026)
[51] J. X. Li and S. Wang, Eur. Phys. J. C **85**(11), 1308 (2025)
[52] Z. Y. Peng and Y. S. Piao, Phys. Rev. D **113**(2), 023544 (2026)
[53] Z. Y. Peng, J. Q. Jiang, H. Wang *et al*., Phys. Rev. D **112**(12), 123519 (2025)
[54] P. J. Wu, T. N. Li, G. H. Du *et al*., Chin. Phys. C **50**(4), 045105 (2026)
[55] C. Fu, D. Lu, and S. J. Wang, Phys. Rev. D **113**(8), L081304 (2026)
[56] L. Feng, T. N. Li, G. H. Du *et al*., Phys. Dark Univ. **52**, 102296 (2026)
[57] F. Y. Zhang, R. Zhai, and L. Y. Chen, Chin. Phys. C **50**(6), 065107 (2026)
[58] W. Yang, C.,H. Wu, and Y. P. Hu, Phys. Lett. B **878**, 140532 (2026)
[59] H. G. Choi, P. Petrov, and S. C. Park, JCAP **04**, 025 (2026)
[60] S. D. Odintsov and V. K. Oikonomou, Phys. Lett. B **870**, 139907 (2025)
[61] J. Kim, X. Wang, Y.-l. Zhang *et al*., JCAP **09**, 011 (2025)
[62] Yogesh, A. Mohammadi, Q. Wu *et al*., JCAP **10**, 010 (2025)
[63] A. Mohammadi, Yogesh, and A. Wang, Phys. Lett. B **872**, 140054 (2026)
[64] A. Addazi, Y. Aldabergenov, D. Berkimbayev *et al*., arXiv: 2512.21167
[65] A. Addazi, Y. Aldabergenov, and S. V. Ketov, Phys. Lett. B **869**, 139883 (2025)
[66] K. G. Zhang, C. Fu, J. F. He *et al*., arXiv: 2604.0214
[67] Q. Y. Wang, Phys. Rev. D **113**(12), L121302 (2026)
[68] M. A. Sabogal, A. J. Iovino, and S. Vagnozzi, arXiv: 2606.31362
[69] Z. Qiu, Y. Pang, and Q. Huang, Sci. China Phys. Mech. Astron. **69**(6), 260413 (2026)
[70] V. K. Oikonomou, Annals Phys. **492**, 170547 (2026)
[71] S. D. Odintsov and V. K. Oikonomou, Nucl. Phys. B **1025**, 117384 (2026)
[72] C. Armendariz-Picon, T. Damour, and V. F. Mukhanov, Phys. Lett. B **458**, 209 (1999)
[73] J. Garriga and V. F. Mukhanov, Phys. Lett. B **458**, 219 (1999)
[74] C. Cheung, P. Creminelli, A. L. Fitzpatrick *et al*., JHEP **03**, 014 (2008)
[75] X. Chen, M.-x. Huang, S. Kachru *et al*., JCAP **01**, 002 (2007)
[76] X. Gao and D. A. Steer, JCAP **12**, 019 (2011)
[77] X. H. Meng and P. Wang, Class. Quant. Grav. **21**, L101 (2004)
[78] C. Fu, P. Wu, and H. Yu, Phys. Rev. D **101**(2), 023529 (2020)
[79] X. M. Kuang and E. Papantonopoulos, JHEP **08**, 161 (2016)
[80] C. Wetterich, Phys. Lett. B **726**, 15 (2013)
[81] C. Wetterich, Phys. Lett. B **736**, 506 (2014)
[82] M. W. Hossain, R. Myrzakulov, M. Sami *et al*., Phys. Rev. D **90**(2), 023512 (2014)
[83] M. W. Hossain, R. Myrzakulov, M. Sami *et al*., Phys. Rev. D **89**(12), 123513 (2014)
[84] M. W. Hossain, R. Myrzakulov, M. Sami *et al*., Phys. Lett. B **737**, 191 (2014)
[85] V. F. Mukhanov and A. Vikman, JCAP **02**, 004 (2006)
[86] S. Unnikrishnan, Phys. Rev. D **78**, 063007 (2008)
[87] S. Unnikrishnan, V. Sahni, and A. Toporensky, JCAP **1208**, 018 (2012)
[88] S. Li and A. R. Liddle, JCAP **10**, 011 (2012)
[89] P. Pareek and A. Nautiyal, Phys. Rev. D **104**(8), 083526 (2021)
[90] S. Lola, A. Lymperis, and E. N. Saridakis, Eur. Phys. J. C **81**(8), 719 (2021)
[91] T. Zhu, A. Wang, G. Cleaver *et al*., Phys. Rev. D **90**(10), 103517 (2014)
[92] M. Liu, T. Y. He, B. Chen *et al*., Phys. Dark Univ. **49**, 102039 (2025)
[93] C.-Q. Geng, M. W. Hossain, R. Myrzakulov *et al*., Phys. Rev. D **92**(2), 023522 (2015)
[94] D. Baumann and D. Green, JCAP **05**, 017 (2012)
[95] G. Cabass, M. M. Ivanov, O. H. E. Philcox *et al*., Phys. Rev. Lett. **129**(2), 021301 (2022)